

# Nickel-based catalysts for non-enzymatic electrochemical sensing of glucose: A review

Filippo Franceschini<sup>a,\*</sup>, Irene Taurino<sup>a,b</sup>

<sup>a</sup> Dept. of Physics and Astronomy (HF), University of Leuven (KU Leuven), 30001, Leuven, Belgium

<sup>b</sup> Dept. of Electrical Eng. (ESAT-MNS), University of Leuven (KU Leuven), 30001, Leuven, Belgium

## ARTICLE INFO

### Keywords:

Nickel  
Glucose sensor  
Sulfides  
Selenides  
Nitrides  
MOF

## ABSTRACT

Nickel-based catalysts are currently the subject of intensive study in the search for novel electrode materials for non-enzymatic glucose sensing. Their strong activity towards glucose electrooxidation and intrinsic resistance to chloride poisoning makes these catalysts ideal candidates for the development of affordable and stable glucose sensors. In this review, the mechanism of glucose electrooxidation at Ni electrodes is described, clarifying the effect of the different phases of Ni on their catalytic activity. Moreover, a brief background on chloride poisoning is provided, supplemented by computational studies. Furthermore, this article details the most intriguing compounds of Ni (selenides, sulfides, nitrates) and the analytical performance of the respective sensors. Additional focus points of this work are multimetallic nanosystems where Ni is a component, and the growing field of conductive metal organic frameworks with Ni centers. This review will be beneficial for researchers who aim at delving deeper into the potential of Ni-based materials for glucose sensing.

## 1. Introduction

Over the last decades, the increasing incidence of Diabetes Mellitus in both developing and affluent countries [1] has further highlighted the need for new approaches to glucose sensing. Currently, most of the commercially available products are still based on the same principle behind the enzymatic biosensor proposed by Clark in 1962 [2,3]. Although enzymatic electrochemical sensors have the potential to be produced at a low cost and be compact, they suffer from a limited functional period which complicates their use for continuous monitoring applications [4]. The poor stability of the signal can chiefly be attributed to fouling by non-target species, and in particular to the use of the enzyme, whose activity progressively reduces over time [5]. Additionally, the enzyme's sensitivity to temperature, pH and humidity changes and the high risk of enzyme leaching increases the complexity of the manufacturing process and imposes more delicate conditions of usage [6]. To overcome these drawbacks, mechanisms of non-enzymatic electrochemical glucose sensing have been studied [5,7,8]. In this regard, nanomaterials play a major part [9]. Different nanostructured electrode materials have been developed over the years and in particular noble metals (Au, Pt, Pd etc.) [10] played a significant role in the advancement towards *fourth-generation* glucose sensors.

Considerable effort has been dedicated in understanding the mechanism of direct electrooxidation at metal electrodes. Accordingly, two models have been proposed: the chemisorption model [11] and the incipient hydrous oxide adatom mediator model [12].

Despite the extensive studies on the oxidation process, the use of bulk noble metals for glucose sensing is limited, due to the presence of many shortcomings [13,14]. First, the competition of anions such as halides for glucose adsorption, leading to catalyst poisoning [15,16]. Secondly, the electrode's degradation as a result of fouling by species commonly found in physiological solutions. Lastly, the much greater cost of noble metals compared to other materials, due to their scarcity and use as assets in the financial system [17].

For these reasons, the research community has focused its attention on finding alternative materials capable of electrooxidizing glucose without being as affected by poisoning and fouling, while costing a fraction of the noble metals. Examples are metal oxides (NiO, CuO, Co<sub>3</sub>O<sub>4</sub> etc.) [18–20], metal sulfides (NiS, FeS<sub>2</sub>, CuS<sub>2</sub>, etc.) [21–23], metal organic frameworks [24–26] and carbon materials (graphene, carbon nanotubes etc.) [27]. Alloying [28], doping [29] and carbon composites [30] are common approaches being explored to fine tune the catalytic activity and/or poisoning resistance.

In particular, in the field of glucose sensing the element nickel has

\* Corresponding author. Celestijnenlaan 200d, 3001, Heverlee, Belgium.

E-mail address: [filippo.franceschini@kuleuven.be](mailto:filippo.franceschini@kuleuven.be) (F. Franceschini).

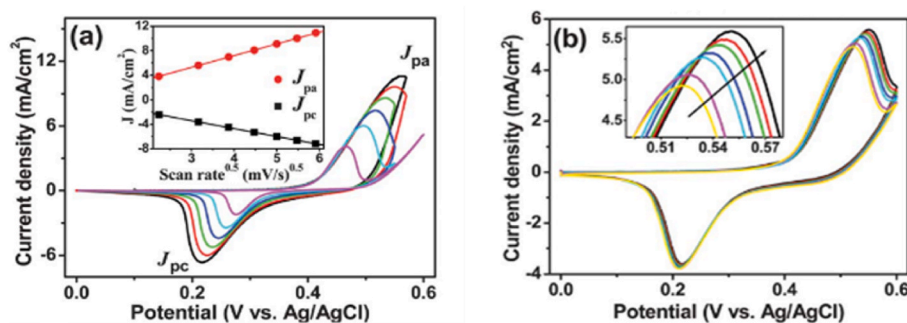


**Fig. 1.** a) Cyclic voltammograms of 500  $\mu\text{M}$  glucose obtained with the 150 nm  $\text{Ni}(\text{OH})_2$ -nitrogen-incorporated nanodiamond ( $\text{Ni}(\text{OH})_2$ -NND) electrode in 0.5 M NaOH solution at scan rates of 5, 10, 15, 20, 25, 30 mV/s. (b) Cyclic voltammograms of the 150 nm  $\text{Ni}(\text{OH})_2$ -NND electrode at a scan rate of 10 mV/s in 0.5 M NaOH in the presence of 50, 100, 150, 250, 350, and 500  $\mu\text{M}$  of glucose. Reproduced from Ref. [38] with permission from the Royal Chemical Society.

shown exceptional potential, finding application in its pure form, in compounds and also recently in conductive metal organic frameworks. Its widespread use can be mainly attributed to the highly oxidizing power of the Ni(II)/Ni(III) couple [31,32] and to its intrinsic resistance to halogen poisoning (both by itself and in combination with noble metals) [33].

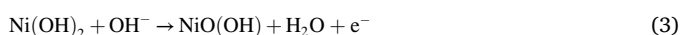
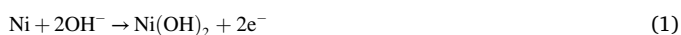
Furthermore, nickel is a naturally occurring element that can be readily found in the environment, existing in over a 100 different mineral forms [34]. It belongs to the transition series with other group 10 elements such as Pt and Pd. Sometimes considered as the “impoverished” sibling of Pt, its high activity towards sluggish reactions in homogeneous [35] and heterogeneous catalysis [36] proves this characterization to be limited. Additionally, the wider availability of Ni makes it vastly more affordable than common noble metal catalysts (e.g., the price of Ni is presently 2500-fold lower than for Au). As a result, more researchers are turning to nickel-based materials for application as either supports or catalysts due to their outstanding yet highly tunable properties.

This review article summarizes the most recent progress in the development of Ni-based non-enzymatic electrochemical glucose sensors. The fundamentals of glucose electrooxidation at Ni electrodes are highlighted, which can in some part be extended to other Ni-based systems. The literature on the chloride poisoning is briefly presented and a possible explanation for its resilience compared to noble metals is proposed. Additionally, the analytical performance of sensors based on Ni compounds, bimetallic nanostructured systems and metal organic frameworks with Ni centers is discussed.

## 2. Electrooxidation of glucose on Ni electrodes in alkaline solutions

The electrochemical oxidation of glucose on Ni electrodes has been reported in numerous studies to occur at the same potential of the Ni(III) oxide formation [37]. Accordingly, the electron transfer appears to be mediated by the  $\text{Ni}(\text{OH})_2/\text{NiO}(\text{OH})$  redox couple. As a consequence, the overall electrocatalytic activity of Ni towards glucose electrooxidation is positively correlated with pH.

In alkaline solutions, the following mechanism has been proposed by Fleischmann and others:



The Nickel(III) acts as a strong oxidant towards glucose (and other organic compounds [32]) by participating in the rate limiting step of the

electrooxidation: the hydrogen abstraction from the  $\text{C}_\alpha$  to the functional group. The irreversible nature of the oxidation reaction is confirmed by the increase in peak current for increasing glucose concentrations limited only to the anodic scan (Fig. 1-a).

To achieve reproducible results, a good strategy is to first perform a few scans of cyclic voltammetry between 0V and 0.7V (vs Ag/AgCl/KCl (3 M) reference electrode), which guarantees the complete conversion of Ni and NiO species to  $\text{Ni}(\text{OH})_2$  and  $\text{NiO}(\text{OH})$  [39].

For the sake of comparison, many researchers evaluate their Ni-based electrodes' performance at pH 13. Nevertheless, an optimization study should always be considered in order to evaluate the hydroxyl concentration that leads to the highest peak current and the lowest background current (current response in the absence of the analyte). In a recent work, Ko et al. [38] proved *via* chronoamperometry that the concentration of NaOH producing the best signal to noise ratio was 0.5 M. Clearly, care should be taken not to generalize their results to other systems having different substrates or additional catalysts.

Two different forms exist for  $\text{Ni}(\text{OH})_2$  ( $\alpha$  and  $\beta$ ) and for  $\text{NiO}(\text{OH})$  ( $\beta$  and  $\gamma$ ) [40]. Visscher and Barendrecht [41] as well as Hahn et al. [42] observed that  $\alpha$ - $\text{Ni}(\text{OH})_2$  slowly transforms in  $\beta$ - $\text{Ni}(\text{OH})_2$  as a result of electrochemical ageing. In particular, the transformation from  $\alpha$ - $\text{Ni}(\text{OH})_2$  to  $\beta$ - $\text{Ni}(\text{OH})_2$  is associated with a shift of the anodic peak position to higher potentials. As a result, for a fixed potential the current density for water oxidation will be reduced for aged electrodes. This polymorphism can account for the diverse electrochemical response of different Ni electrodes.

## 3. Selectivity and non-enzymatic glucose sensors

One of the main disadvantages of non-enzymatic glucose sensors is the lack of a selective recognition mechanism. Nickel-based catalysts and non-enzymatic glucose sensors as a whole, once polarized can oxidize many other molecules in addition to glucose. This can be attributed to the easily accessible catalytic sites (e.g.  $\text{NiOOH}$ ) which on a flat electrode surface can be reached by small and large molecules alike. As a result, the electrode's current response may poorly correlate with the real serum glucose concentration. In particular, the main interferents are reportedly: ascorbic acid, uric acid, acetaminophen and dopamine [43]. Acetaminophen and dopamine can be especially problematic when their oxidation products have an affinity for the electrode surface (usually carbon-based) because they can effectively block the catalytically active sites [44,45]. Other interferents include mono and disaccharides such as fructose and sucrose, which possess a similar chemical structure to glucose. Disaccharides do not exist in the bloodstream [46], since they get separated into their constituents by enzymes during digestion (e.g. sucrose gets separated by sucrase into glucose and fructose). However, in the case of fructose its blood concentration is usually 10–1000 times lower than that of glucose [47], thus posing no particular issue from an analytical standpoint.

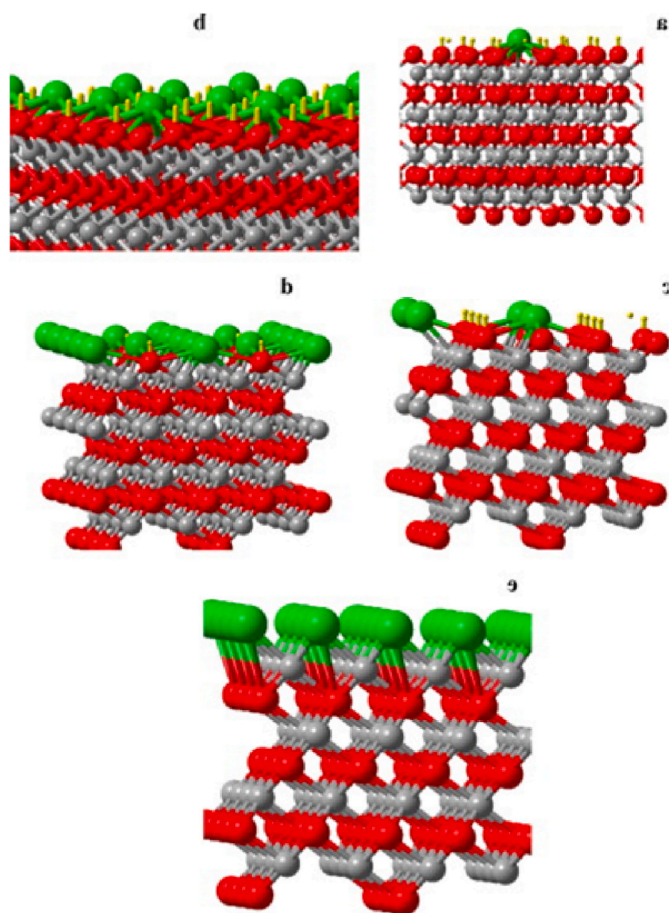


Fig. 2. OH substitution by Cl: (a) 6%, (b) 25%, (c) 50%, (d) 75% and (e) 100% proportion substitution. Grey atoms, Ni; red, O; green, halide; yellow, hydrogen). Reproduced from Ref. [63] with permission from Elsevier. (For interpretation of the references to colour in this figure legend, the reader is referred to the Web version of this article.)

Overall, nickel-based non enzymatic glucose sensors can achieve a satisfactory level of selectivity and this can be attributed to a number of reasons. First of all, the concentration of interferents in the blood serum is usually more than 10 fold lower than that of glucose (which for healthy individuals is around 4 mM [48]). Accordingly, even supposing to oxidize the interferents with the same kinetic rate, this would at most cause a 10% uncertainty in the current signal. Second of all, the majority of the proposed electrode configurations in the literature involve some measure of surface nanostructuring [9], which can act as a size control for molecules larger than glucose. Additionally, the high degree of hydroxylation of Ni-based electrodes renders the surface extremely hydrophilic, which naturally repels hydrophobic species such as most fouling agents [49]. Moreover, the electrochemical technique being used also has an impact. Accordingly, good selectivity can be achieved in certain systems with potentiostatic approaches (chronoamperometry) by choosing a potential at which glucose is oxidized, but not the interferents. Lastly, the use of membranes (e.g. Nafion) has been shown to effectively protect the surface from fouling, while maximizing the overall sensor's selectivity mostly through a size selection mechanism [50,51].

#### 4. Halide poisoning and nickel's resistance to Cl<sup>-</sup>

The chloride ion (Cl<sup>-</sup>), with a molar mass of 35.45 g/mol, is the most abundant anion in the human serum with a concentration around 97–107 mM [52]. It plays a significant role in the fluid homeostasis,

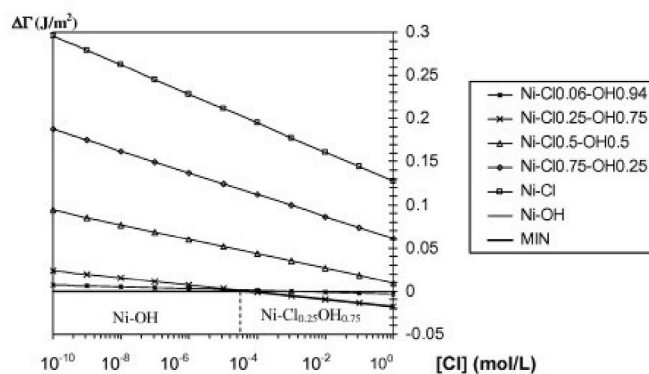


Fig. 3. Interface free energy variations (J/m<sup>2</sup>) (referenced to the free energy of the hydroxylated NiO surface) obtained for the several substitution proportions of hydroxyls by Cl<sup>-</sup>. Reproduced from Ref. [63] with permission from Elsevier.

electrolyte balance, conservation of electrical neutrality and acid base status [53].

Its significant concentration in the extracellular fluid is well known to impair the performance of non-enzymatic glucose sensors in a process referred to as *halide poisoning*, where the surface-active sites of the catalyst are being blocked. Noble metals, such as Pt and Au, are reported to be particularly affected by halide poisoning for glucose and methanol electrooxidation [54–57]. The reason for the loss of catalytic activity has been attributed to the specific adsorption of Cl<sup>-</sup>. Moreover, the presence of chlorides causes the formation of soluble species instead of an oxide layer from Au [16,58], inevitably leading to corrosion. Similarly, electrochemical cycling in chloride rich solutions is known to cause Pt etching [15].

Conversely, the surface of metals such as Ni spontaneously forms a passivation film composed of an inner NiO with an hydroxylated outer layer, which protects it against corrosion [59]. In certain conditions, the interaction with halides can still lead to the breakdown of the passivation film, and the subsequent corrosion by pitting.

Nonetheless, NiOx is drastically less susceptible to poisoning compared to noble metals and the reason for this has generally been attributed to a difference in adsorption energy of the halide ion on the different surfaces [60,61]. A deep evaluation of the poisoning resistance of NiOx electrodes was first performed by El-Rafaei and colleagues [33], who recorded the glucose electrooxidation peak in 0.5 M NaOH before and after the addition of 0.1 M Cl<sup>-</sup>. After chloride addition, the peak current decreased to a minimum at the 4th cycle (losing 4% of the initial value), and then it increased again almost to the original value after the 15th cycle. This behavior may be explained by the low absorbability of Cl<sup>-</sup> ions, and possibly by the high reversible oxidation potentials of the Cl<sub>2</sub>/Cl<sup>-</sup> couples [62].

A deeper understanding of the mechanisms at play is provided by computational approaches. In a pivotal work, Bouzoubaa et al. [63] described the interaction of an hydroxylated defect-free NiO(111) surface with different halides (F<sup>-</sup>, I<sup>-</sup>, Cl<sup>-</sup>, Br<sup>-</sup>).

Fig. 2 shows the modeled slab for different OH- substitutions by halide ions X<sup>-</sup>.

In particular, as the chloride coverage increases and the Cl<sup>-</sup> progressively substitutes more OH<sup>-</sup> groups, the lateral anion-anion repulsions gradually reduce the OH<sup>-</sup> substitution energy (becoming endothermic at more than 75% substitution). This result is confirmed by previous studies [64]. Moreover, since the ionic radius of Cl<sup>-</sup> is larger than that of OH<sup>-</sup>, the NiCl bond length is larger than that of NiO, thus leading to a splitting in the mixed topmost plane.

Fig. 3 may be read as follows: at low chloride concentrations (<10<sup>-4</sup> M) the NiOH termination is the most energetically favorable, whereas above 10<sup>-4</sup> M the 25% OH<sup>-</sup> substitution is the most stable configuration even at high Cl concentrations, due to the strong anionic repulsion

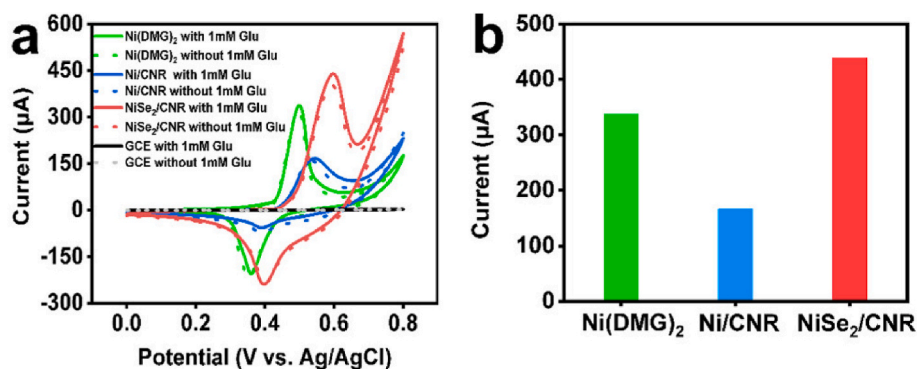


**Fig. 4.** (a) CV curves of the bare GCE, Ni(DMG)<sub>2</sub>, Ni/Carbon nanorods(CNR), and NiSe<sub>2</sub>/CNR-modified GCEs in the presence of 0.1 M NaOH with or without 1 mM glucose; (b) corresponding histogram of current responses of Ni(DMG)<sub>2</sub>, Ni/CNR, and NiSe<sub>2</sub>/CNR. Reproduced from Ref. [75] with permission from the American Chemical Society.

between Cl ions. This calculation may explain why NiOx electrodes are intrinsically resilient to chloride poisoning: approximately three quarters of surface hydroxyl groups are maintained, which during polarization in an alkaline electrolytes can still give rise to the highly oxidizing Ni(III).

## 5. Nickel compounds

### 5.1. Nickel selenides

The small difference in electronegativity between Ni ( $\chi = 1.91$ ) and Se ( $\chi = 2.55$ ) allows the formation of different nickel selenides [65]. A wide range of phases have been reported to be stable at room temperature: NiSe<sub>2</sub>, NiSe, and Ni<sub>3</sub>Se<sub>2</sub>. Based on the prediction of Horn and Goodenough's [66], an increase in the covalency of the metal-oxygen bond significantly influences the binding of oxygen-related intermediate species, which in alkaline solutions are important pathways to glucose electrooxidation.

In the field of electrocatalysis of the different nickel selenides, a prominent role is played by Ni<sub>3</sub>Se<sub>2</sub> and NiSe<sub>2</sub>, which boast a narrow band gap and high conductivity, making them intriguing candidates for non-enzymatic glucose sensors. Moreover, metal selenides possess higher electrical conductivity, compared to the respective oxides and sulfides, due to the strong metallic character of selenium [67,68]. Different selenylation approaches have been proposed, but most are based on techniques such as hydrothermal [69] or solvothermal [70] synthesis, electrodeposition [71], solution chemical process [72] or solid state synthesis [73]. Although the literature on nickel selenides for glucose sensing is still scarce, the current reports are highly promising. The first study on the use of NiSe<sub>2</sub> as an electrode modifier for OH<sup>-</sup>

mediated glucose electrooxidation was done by Mani et al. [74]. Here, the researchers employed a hydrothermal synthesis method and then a drop cast of the nanosheets in an alcoholic dispersion on a glassy carbon electrode. The authors proposed the following redox process for the electrode in the absence of glucose in alkaline solution:



During the cyclic voltammogram the Ni(III) and Se(II) species are oxidized to Ni(IV) and Se(III), which readily oxidize glucose to gluco-lactone. The enhancement in the electrocatalytic activity may be attributed to the ability of the Se constituent to increase the charge transport efficiency between the Ni center and the electrode substrate. Although reasonable, in the absence of a Ni electrode control such assertions still need to be verified. The calculated sensitivity for the electrode after amperometric calibration in 0.1 M NaOH was limited to 5.6  $\mu\text{A mM}^{-1} \text{cm}^{-2}$  with a *limit of detection* (LOD) of 0.023  $\mu\text{M}$ .

In order to improve the electron transfer capabilities of nickel selenide-based electrodes, some researchers have combined them with carbon nanostructures. For instance, in a recent work, Xu et al. [75] fabricated a hierarchical electrode composed of carbon nanorods and NiSe<sub>2</sub>, synthesized through a facile thermal route. After dispersion in a Nafion solution, it was drop cast on a glassy carbon electrode. The reported sensitivity was 3636  $\mu\text{A mM}^{-1} \text{cm}^{-2}$  with a LOD of 0.38  $\mu\text{M}$ , after amperometric calibration in 0.1 M NaOH. Evidently, the mechanical stabilization of the NiSe<sub>2</sub> nanosheets with a conductive membrane greatly improves the overall performance of the sensor. Fig. 4 clarifies the effect of the carbon nanorod incorporation, having a significant and positive influence on the current increment as a result of glucose addition.

While electrode fabrication procedures such as drop casting and thin

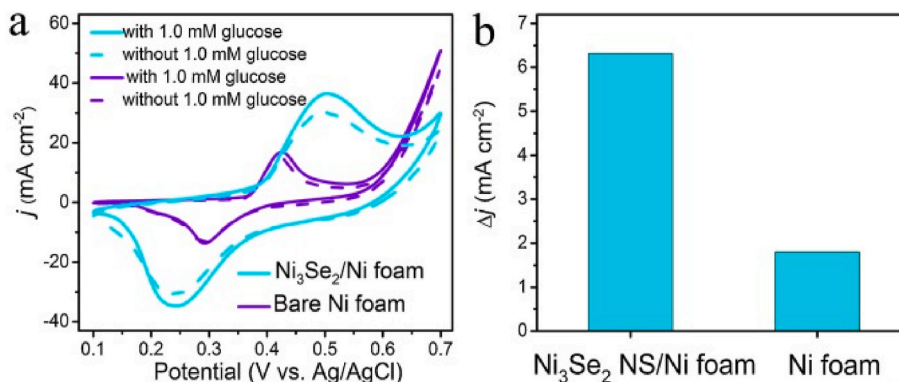


**Fig. 5.** (a) CVs of Ni<sub>3</sub>Se<sub>2</sub> NS/NF and bare Ni foam in 0.5 M NaOH in the absence (dash curves) and presence (solid curves) of 1.0 mM glucose at a scan rate of 20 mV s<sup>-1</sup>. (b) The bar chart of comparison of current density increments for different electrodes. Reproduced from Ref. [77] with permission from Elsevier.

**Table 1**  
Comparison table for nickel selenides-based electrochemical non-enzymatic glucose sensors.

Electrode	Electrolytic solution	Linear range ( $\mu\text{M}$ )	LOD ( $\mu\text{M}$ )	Sensitivity ( $\mu\text{A } \mu\text{M}^{-1} \text{cm}^{-2}$ )	Ref.
NiSe <sub>2</sub> -NS/GCE	0.1 M NaOH	0.099–1252	0.023	5.6	[74]
NiSe <sub>2</sub> /CNR	0.1 M NaOH	0.5–411	0.38	3636	[75]
Ni <sub>3</sub> Se <sub>2</sub> NS/NF	0.1 M NaOH	0.25–2835	0.04	5962	[77]
		2.835–6.335		4362	
NiSe NW	0.5 M NaOH	5–3000	5	5	[78]
NiSe <sub>2</sub> /Cellulose	0.1 M NaOH	100–1000	25	0.25	[79]

film coating are common in the literature, they are time consuming and require the use of polymeric binders in order to fix the catalyst on the electrode's surface. In these cases, the catalytic active centers can get significantly blocked by the polymer, thus hindering the electron transfer capabilities of the electrode as a whole [76].

A more scalable solution, which has been explored not only for Ni selenides, is the synthesis of the active catalyst directly from the corresponding metal (e.g., Ni). In this way, there is no need for a membrane to guarantee the direct catalyst-electrode contact, which, as previously stated, impairs the electrical conductivity.

As an example, Ma et al. [77] fabricated through hydrothermal routes Ni<sub>3</sub>Se<sub>2</sub> nanosheets (NS) supported on a Ni foam, with a reported sensitivity of 5962  $\mu\text{A } \text{mM}^{-1} \text{cm}^{-2}$  and a LOD of 0.04  $\mu\text{M}$ . Fig. 5 highlights the improvement in the current density ( $\Delta j$ ), going from a bare Ni foam to a Ni<sub>3</sub>Se<sub>2</sub>/Ni Foam. The authors attributed the increase in sensitivity to the synergistic interaction between the Ni<sub>3</sub>Se<sub>2</sub> nanosheets and the Ni support.

Table 1 lists all the non-enzymatic glucose sensors described in this section.

## 5.2. Nickel sulfides

Compounds of Ni with chalcogenides for glucose sensing are not solely limited to selenides. Ni sulfides have been closely investigated as well. The main reported advantages of these materials are their high redox ability, good electrical conductivity and thermomechanical stability [80]. Electronic and band structure calculation suggest that as the ratio of S to Ni increases, the Ni *d*-band centers become more negative and the S *p*-band centers become more positive [81]. The presence of a band gap between Ni *d*-band and the S *p*-band explains why nickel sulfides are generally less conductive than pure Ni. It has been shown that the phase of nickel sulfide has a meaningful effect on the catalytic activity for the hydrogen evolution reaction [82]. As of now, no studies have definitively clarified its impact towards glucose electrooxidation.

Nickel sulfides can exist in different crystalline structures and stoichiometric ratios, such as Ni<sub>3</sub>S<sub>2</sub>, NiS, NiS<sub>2</sub>, Ni<sub>3</sub>S<sub>4</sub>. They find application in different fields, ranging from dye-sensitized solar cell [83] to supercapacitors [84] and electro(photo)catalytic oxygen/hydrogen evolution [28,29]. The current scientific research on nickel sulfides for glucose

sensing is mainly focused on exploring the catalyst-support interaction which provides the greatest sensitivity, stability and reproducibility. The first work on an electrodeposited NiS film was performed by Kannan et al. directly on *indium tin oxide* (ITO) electrodes [85]. The chosen synthesis method was straightforward and easily scalable, granting a sensitivity in 0.1 M NaOH of 7430  $\mu\text{A } \text{mM}^{-1} \text{cm}^{-2}$ .

In alkaline solution the proposed reversible redox reaction is the following [86]:



Given that the morphology has a strong effect on the catalytic activity, the majority of the published research works report catalyst nanostructuring. Accordingly, hollow spheres of  $\alpha$ -NiS have been studied due to their good electrocatalytic activity and stability, ease of synthesis, and environmental compatibility [87]. Interestingly, the authors observed a significant difference between the  $\alpha$ -NiS and the  $\beta$ -NiS hollow spheres, with the former leading to a stronger electrocatalytic response. However, the abovementioned sensor had a sensitivity of only 155  $\mu\text{A } \text{mM}^{-1} \text{cm}^{-2}$ . This was likely the result of aggregation, which reduced the active sites and the non-exceptional electrical conductivity of NiS. To overcome these obstacles many authors make use of a conductive matrix, such as functionalized carbon black [88]. Relatedly, Ni<sub>3</sub>S<sub>2</sub>/carbon composites have also been fabricated, as done by Lin and colleagues [89], by using an hydrothermal method where the carbonaceous matrix consisted of multiwalled carbon nanotubes.

With an interesting approach, Meng et al. [90] grew a Ni<sub>3</sub>S<sub>2</sub> nanoworm (NW) network directly on a poly (3,4-ethylenedioxythiophene)-reduced graphene oxide hybrid films (PEDOT-rGO HF) modified on glassy carbon electrode. A schematic of the fabrication process is illustrated in Fig. 6. The sensor showed good sensitivity (2123  $\mu\text{A } \text{mM}^{-1} \text{cm}^{-2}$ ) and low LOD (0.48  $\mu\text{M}$ ), that the authors attributed to a combination of high surface area, morphology, hydrophilic nature allowing easy OH<sup>-</sup> adsorption and good coupling between the different electrode layers.

As of now, one of the most promising technological methods is to directly grow the nickel sulfide catalyst directly on a nickel foam. For instance, Huo et al. [91] fabricated a 3D Ni<sub>3</sub>S<sub>2</sub> nanosheet array supported on a Ni foam by hydrothermal synthesis using nickel nitrate and thiourea. After amperometric calibration in 0.5 M NaOH, the measured

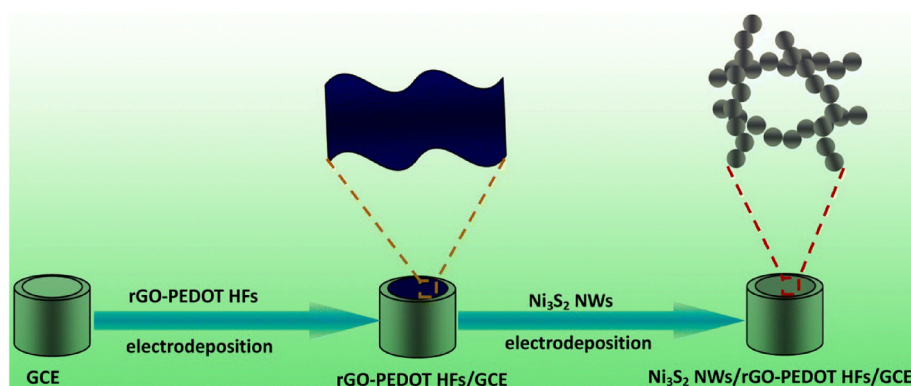


**Fig. 6.** Schematic illustration of the synthesis process for Ni<sub>3</sub>S<sub>2</sub> NWs/PEDOT-rGO HF/GCE. Reproduced from Ref. [90] with permission from Springer Nature.

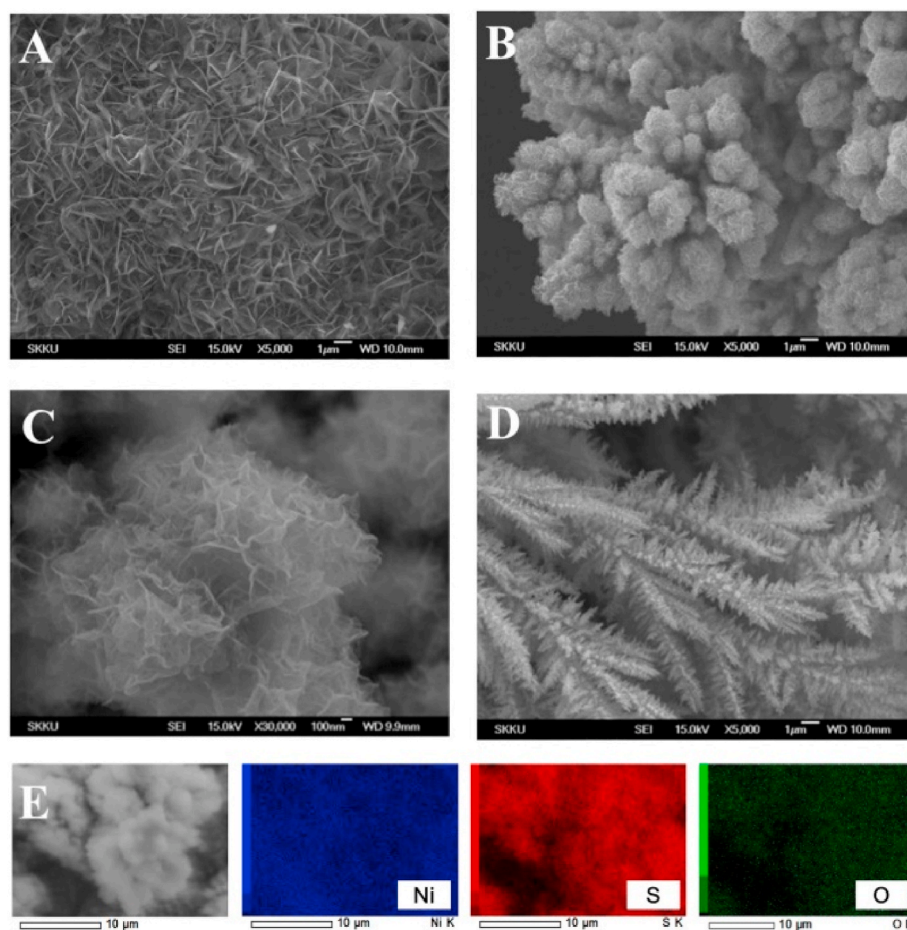


**Fig. 7.** SEM images of nickel sulfide using various reaction medium:  $\text{Ni}_3\text{S}_2\text{-Et}$  (A),  $\text{Ni}_3\text{S}_2\text{-Et/W}$  (B),  $\text{Ni}_3\text{S}_2\text{-Et/W}$  with high magnification (C), and  $\text{Ni}_3\text{S}_2\text{-W}$  (D), and EDS maps of nickel, sulfur, and oxygen from  $\text{Ni}_3\text{S}_2\text{-Et/W}$  (E). Reproduced from Ref. [92] with permission from Elsevier.

**Table 2**

Comparison table for nickel sulphides-based electrochemical non-enzymatic glucose sensors.

Electrode	Electrolytic solution	Linear range ( $\mu\text{M}$ )	LOD ( $\mu\text{M}$ )	Sensitivity ( $\mu\text{A mM}^{-1} \text{cm}^{-2}$ )	Ref.
NiS/ITO	0.1 M NaOH	5–45	0.32	7530	[85]
3D $\text{Ni}_3\text{S}_2$	0.5 M NaOH	0.005–3.0	1.2	6148	[91]
$\text{Ni}_3\text{S}_2$ /MWCNT	0.1 M NaOH	30–500	1	3345	[89]
$\alpha$ -NiS spheres	0.1 M NaOH	0.125–2000	0.12	155	[87]
f-CB/NiS/GCE	0.1 M NaOH	0.125–268 268–1781	0.02	1223	[88]
NiS/r-GO	0.1 M NaOH	0.5–1700	0.1	–	[93]
$\text{Ni}_3\text{S}_2$ NW/GCE	0.1 M NaOH	15–9105	0.48	2123	[90]
$\text{Ni}_3\text{S}_2$ /NF	0.5 M NaOH	0.5–3000	0.82	16460	[92]

sensitivity was  $6148 \mu\text{A mM}^{-1} \text{cm}^{-2}$ , with a LOD of  $1.2 \mu\text{M}$ , mainly ascribed to the open channel structure, combined with a fast electron and ion transport. Alternatively, as illustrated in a similar work by Kim et al.,  $\text{Ni}_3\text{S}_2$  nanostructures can be hydrothermally grown on a Ni-foam by having it react with thioacetamide in an alcohol and water medium [92]. By adjusting the solvent composition, a hierarchical cauliflower-like structure was obtained (Fig. 7b). The sensor showed superior sensitivity ( $16\,460 \mu\text{A mM}^{-1} \text{cm}^{-2}$ ) and good LOD ( $0.82 \mu\text{M}$ ) in a 0.5 M NaOH solution.

Table 2 describes the detection parameters of non-enzymatic glucose sensors based on nickel sulfides.

### 5.3. Nickel nitrides

Nickel nitride ( $\text{Ni}_3\text{N}$ ) has recently shown to be a promising electrocatalyst for glucose sensing.  $\text{Ni}_3\text{N}$  is a low temperature solid state phase at the boundary between the hcp and hcp + fcc zones, where the nitrogen atoms occupy the octahedral interstitial sites of the nickel lattice in a way that minimizes the N–N interactions [94].

Calculated *Density of States* (DOS) studies indicate that bulk  $\text{Ni}_3\text{N}$  is intrinsically metallic and that the carrier concentration can be additionally enhanced when dimensional confinement was applied along with nanoscale structure [95].

Accordingly, the nitridation process induces a contraction in the d-band near the Fermi level, thus favorably changing the electronic structure for catalytic purposes.

Different nitridation techniques are reported in the literature, such as ammonolysis in a  $\text{NH}_3$  atmosphere [96], reactive physical vapor deposition in  $\text{N}_2$  [97], direct liquid injection chemical vapor deposition with  $\text{NH}_3$  as a co-reactant [98], nitrogen ion implantation [99], plasma based nitridation [100] or a solvothermal process with highly reactive azide or hydrazine [101,102]. When going from bulk to nanostructured materials, multiple stoichiometries of nickel nitride have been reported (e.g.,  $\text{NiN}$ ,  $\text{Ni}_2\text{N}$ ,  $\text{Ni}_4\text{N}$ ,  $\text{Ni}_8\text{N}$ ), due to the fact that phase boundaries can change when the characteristic size is at the nanoscale [103]. The first investigation of  $\text{Ni}_3\text{N}$  as a glucose electrocatalyst was done by Xie et al. [104]. The authors synthesized nickel nitride nanosheets on a Ti mesh by ammonolysis of a previously deposited Ni layer. The sensor after amperometric calibration in 0.1 M NaOH displayed a very high sensitivity of  $7688 \mu\text{A mM}^{-1} \text{cm}^{-2}$  and a LOD of  $0.06 \mu\text{M}$ . However the linear

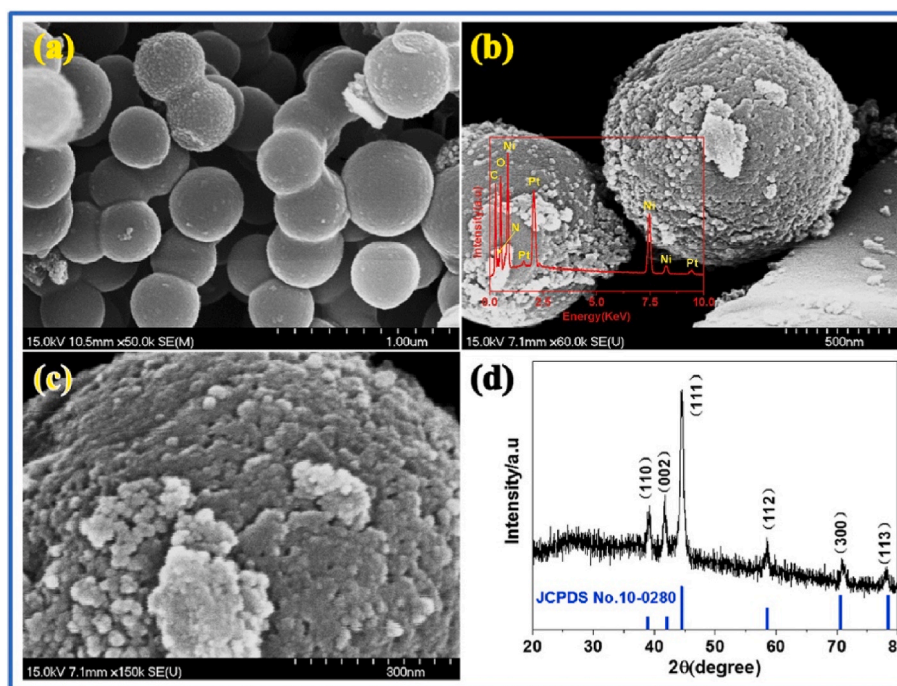


**Fig. 8.** SEM images of (a) carbon spheres and (b), (c)  $\text{Ni}_3\text{N}/\text{N}$ -doped carbon spheres. (d) XRD pattern of  $\text{Ni}_3\text{N}/\text{N}$ -doped carbon sphere. Insert in b is the EDS pattern. Reproduced from Ref. [111] with permission from Elsevier.

**Table 3**

Comparison table for nickel nitrides-based electrochemical non-enzymatic glucose sensors.

Electrode	Electrolytic solution	Linear range ( $\mu\text{M}$ )	LOD ( $\mu\text{M}$ )	Sensitivity ( $\mu\text{A mM}^{-1} \text{cm}^{-2}$ )	Ref.
$\text{Ni}_3\text{N NS}/\text{Ti}$	0.1 M NaOH	0.2–1500	0.06	7688	[104]
$\text{Ni}_3\text{N}-\text{C}$	0.1 M NaOH	0.001–1750 1750–9180	0.05	1620 856	[109]
$\text{Ni}_3\text{N}/\text{NCS}$	0.1 M NaOH	1–3000 3000–7000	0.1	2024 1256	[111]
$\text{Ni}_3\text{N}-\text{Co}_3\text{N}$	0.1 M NaOH	0.1–4000	0.03	4418	[112]
$\text{Ni}_3\text{N}/\text{GA}$	0.1 M NaOH	0.1–7645	0.04	906	[113]
$\text{NiCo}_2\text{N}$	0.1 M NaOH	3–7150	0.05	1803	[114]
$\text{Ni}_3\text{N}/\text{C}$	0.1 M NaOH	1–3000	0.3	783	[115]

range was only up to 1.5 mM, which limits its potential application since the usual blood glucose concentration is around 4–7 mM [105].

As seen with nickel selenides (Section 4.1) and sulfides (Section 4.2), and many other catalytic systems [106–108] the integration of a catalyst, such as  $\text{Ni}_3\text{N}$ , in a conductive carbonaceous matrix can lead to significant enhancements in the sensing capabilities due to the well-known improvements in the electron transfer afforded by carbon materials. In this regard, Liu et al. [109] investigated how a change in the structural parameters of different carbon matrices affected the electrocatalytic activity of a  $\text{Ni}_3\text{N}$  nanosheet/carbon electrode as a whole. The authors concluded that a hollow/tubular 3D porous architecture leads to the best sensing performance towards glucose, due to a greater dispersion of the nanosheets in the inner and outer walls of the carbon fibers. The calculated sensitivity in 0.1 M NaOH was  $1620 \mu\text{A mM}^{-1} \text{cm}^{-2}$  until 1.75 mM and  $856 \mu\text{A cm}^{-2} \text{mM}^{-1}$  (from 1.75 to 9.18 mM), with a LOD of 0.05  $\mu\text{M}$  for the lower concentration range.

To further increase the sensing performance of composite  $\text{Ni}_3\text{N}/\text{C}$  carbon electrodes, a current trend is to work on improving the synergy between the carbon matrix and the nickel nitride catalyst. Nitrogen doping of carbon materials allows to fix the metal sites and to facilitate the catalytic process by regulating the electronic structure of the carbon

matrix [110]. In a recent work, Chen et al. [111] successfully fabricated a sensor based on nickel nitride decorated nitrogen doped carbon spheres ( $\text{Ni}_3\text{N}/\text{NCS}$ ). Fig. 8 shows the morphological details of the bare and modified N-doped carbon nano spheres, and also the XRD spectrum of the synthesized material. A facile, eco-friendly one pot nitridation process was employed and after amperometric calibration in 0.1 M NaOH the calculated sensitivity was  $2024.18 \mu\text{A mM}^{-1} \text{cm}^{-2}$  (up to 3 mM) and  $1256.98 \mu\text{A mM}^{-1} \text{cm}^{-2}$  (from 3 to 7 mM) with respective LOD of 0.1  $\mu\text{M}$  and 0.35  $\mu\text{M}$ .

The sensing parameters of the above-described nickel nitride-based sensors are listed in Table 3.

## 6. Bimetallic nickel-based nanomaterials

A commonly employed strategy to maximize the electrode's sensitivity is to introduce nanoparticles in the design, in order to take advantage of their high specific surface area and augment the number of active sites. A fairly recent avenue for glucose sensing is represented by bimetallic alloy nanomaterials, which by definition are comprised of two or more metals. Due to synergistic interactions, bimetallic nanomaterials are considered to be more electroactive than their monometallic counterpart [116,117]. Depending on the metal combination, significant improvements have been reported in terms of sensitivity, stability, biocompatibility and specificity due to biomimetic behavior [118]. The change in reactivity of a metal as a result of alloying can either be due to a change of the electronic structure, increased number of possible bonding geometries for adsorbates, or more indirectly, due to a change in the lattice parameters [119]. In general, a useful, albeit simple, descriptor for a metal's reactivity has been recognized to be the position of  $d$ -band center  $\epsilon_d$ . The higher (lower) the  $d$ -band center, the stronger (weaker) the affinity of an adsorbate to the metal site [120–122]. As a molecular adsorbate interacts with the metal's  $d$ -band it gives rise to bonding and antibonding molecular orbitals. As a consequence of alloying an upward (downward) shift in the metal  $d$ -band is produced, which leads to a decreased (increased) filling of the metal-adsorbate anti-bonding orbitals. It should be noted that there are exceptions to this rule [123], and more refined models that take into

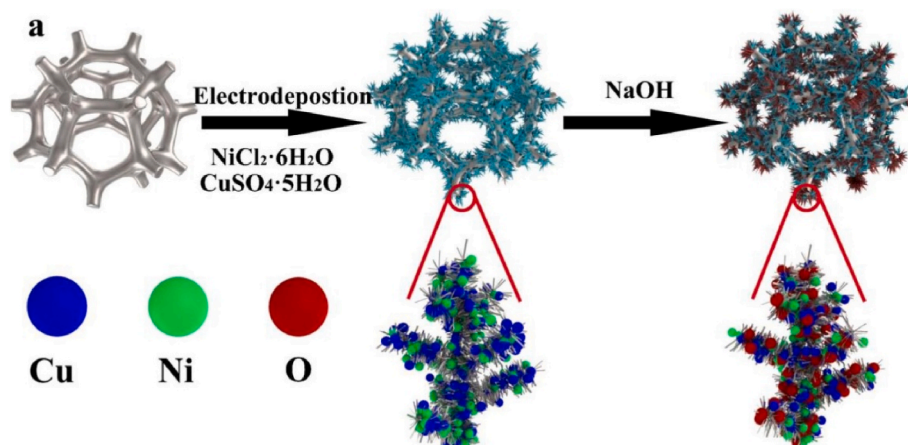


Fig. 9. Schematic illustration of the fabrication process of Cu-Ni/NF electrode. Reproduced from Ref. [138] with permission from Elsevier.

account the shape of the *d*-band have been proposed [124].

The main synthetic methods for Ni-based bimetallic nanostructures are co-reduction [125,126], thermal decomposition [127], seed mediated growth [128], galvanic replacement reaction [129] and electrodeposition [130–132].

The tendency of Ni to oxidize complicates its synthesis in aqueous solutions [133]. An additional hurdle arises due to the magnetic properties of Ni nanoparticles, causing them to cluster together. For this reason there are few reports on the synthesis of monodispersed size distributions for Ni nanoparticles [134,135].

Due to the strong electrocatalytic activity of both copper and nickel in alkaline solution towards glucose electrooxidation [136,137], many researchers have tried to explore how these two metals interact at the nanoscale and how their catalytic activity may change as a result. In a recent study, Wei et al. [138] developed a dendritic Cu@Ni on a Ni foam (NF) electrode for glucose sensing through a facile electrodeposition method. A schematic representation of the system is shown in Fig. 9.

The sensor, after amperometric calibration in 0.1 M NaOH, showed a very high sensitivity of  $11340 \mu\text{AmM}^{-1}\text{cm}^{-2}$  with a LOD of  $2 \mu\text{M}$ . NiO (OH) and CuO(OH) both contribute to a single anodic peak, due to the closeness of their respective oxidation potentials, as also observed in a similar work by Bilal et al. [139]. The strong electrochemical response

was attributed to the synergistic interaction the between oxide shell and the conductive metal core, combined with the high surface area allowing easy glucose diffusion. The investigation of Lin et al. [140] on electrodeposited Ni and Cu nanoparticles on multiwalled carbon nanotubes shed light on two important aspects. First, that the multiwalled carbon nanotubes provide a large conductive area onto which Ni and Cu ions can electrodeposit without competing, thus leading a more ordered and active structure. Secondly, there is a ratio of Cu:Ni which gives the highest glucose oxidation current increment, which was observed to be 1:1.

Analogously, Ammara et al. explored the combination of a Ni-Cu nanocomposite with carbon nanotubes, by sequential electrodeposition on electrophoretically deposited carbon nanotube film [141]. In this way, the oxidation of Cu and Ni is lessened, while guaranteeing good mechanical stability and improved electrical conductivity through the formation of a percolation path. Here, the researchers also noted that the ideal ratio Ni:Cu to be 1:1.

In a recent work, Xu and colleagues [142] fabricated through a one-step hydrothermal synthesis method Ni-Cu bimetallic alloy nanoparticles on reduced graphene oxide. Surprisingly, after running an optimization study on the molar ratio of Ni:Cu, the strongest sensitivity was associated with a 4:1 ratio, in contradiction with the results of Lin

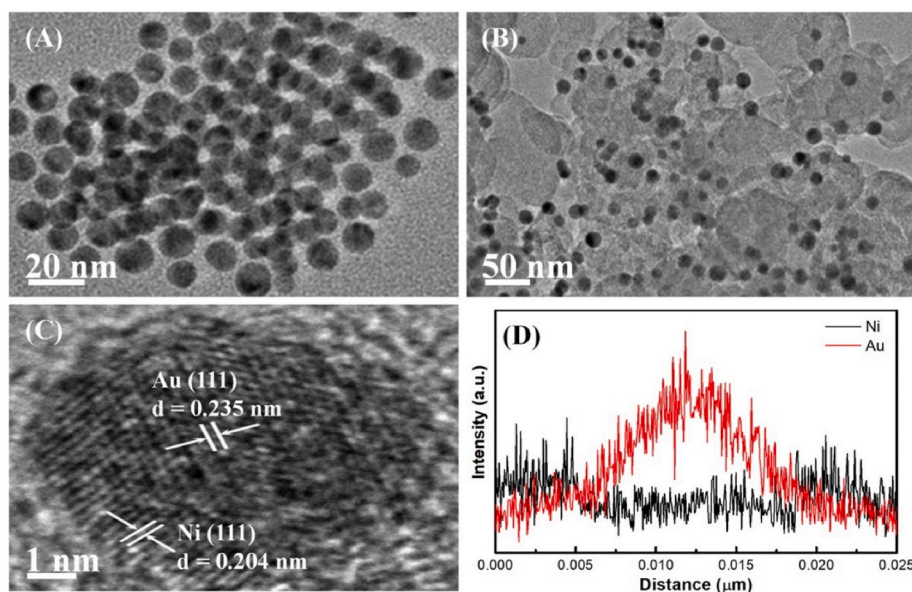


Fig. 10. TEM images of core-shell Au@Ni nanoparticles (A) and Au@Ni/C samples (B); HRTEM image of a single Au@Ni nanoparticle on carbon substrate (C); the line scanning analysis of a single Au@Ni nanoparticle (D). Reproduced from Ref. [148], under CC BY 4.0.

**Table 4**

Comparison table for electrochemical non-enzymatic glucose sensors based on bimetallic nickel-based nanomaterials.

Electrode	Electrolytic solution	Linear range ( $\mu\text{M}$ )	LOD ( $\mu\text{M}$ )	Sensitivity ( $\mu\text{A mM}^{-1} \text{cm}^{-2}$ )	Ref.
Cu–Ni/NF	0.1 M NaOH	1–600	2	11340	[138]
PANI@CuNi	0.1 M NaOH	100–5600	0.2	1030	[139]
Ni–Cu/ MWCNT/ ITO	0.1 M NaOH	0.02–800 2000–8000	0.025	2633 2437	[140]
Ni–Cu/CNT/ FTO	0.1 M NaOH	20–4500	2	1836	[141]
Ni–Cu/rGO	0.1 M NaOH	0.01–30	0.005	1754	[142]
Au@Ni	0.1 M NaOH	100–10000	15	23	[148]
Ni–Au@FTO	0.1 M NaOH	5–3500 3500–7000	0.7	893 554	[144]
Ni–Au/Cpap	0.1 M NaOH	1–3000	0.2	4035	[145]
Ni–Au NW/ ITO	0.2 M NaOH	0.25–2000 2000–5500	0.1	3372 1906	[146]
Au–Ni/BDD	1 M NaOH	20–2000 2000–9000	2.6	157 61	[147]
Ni–Pt NS/ Cpap	0.1 M NaOH	1–10800	0.4	2225	[150]
Ag–Ni/GCE	0.1 M NaOH	1–10 20–107	0.49	–	[151]

et al. [140] and Ammara et al. [141]. In fact, a 1:1 ratio caused a decrease in the sensitivity compared to the bare metal surfaces. The difference in the optimum ratio between the studies is not trivial to explain, but may be due to the different synthetic methods being employed. Possibly, co-electrodeposition might cause the blocking of active sites of Cu at lower molar ratios, compared to hydrothermal methods.

Bimetallic nanostructured systems composed of Ni and a noble metal are a promising solution to the current limitations of pure noble metal electrodes for glucose sensing: namely, the sensitivity to chlorides, which impairs their long term stability [16], and their high cost. Moreover, the addition of a second metal can modulate the catalytic activity and facilitate the reactant adsorption and product desorption, as implied above.

Simultaneously, integrating a noble metal to a Ni electrode produces two main beneficial effects. First, it allows to extend the sensors' range of activity to neutral pH. This is because noble metals (such as Pt, Au) are able to directly electrooxidize glucose without the need for a high concentration of solution hydroxyls in the initial rate-limiting step of  $\text{C}_1$  dehydrogenation [43,143]. Secondly, it causes an increase in the electrical conductivity to the bare Ni electrode. In particular, many authors [144–147], have explored the combination of Au and Ni for electrochemical glucose sensors, noting the presence of synergistic interactions between the two metals.

As an example, the group of Yang synthesized spherical Au@Ni nanoparticles with a core-shell structure through a seed-mediated growth in oleylamine [148]. The core shell structure of the nanoparticles can be clearly appreciated in the TEM image shown in Fig. 10c. The oxidation of glucose on core-shell Au@Ni nanostructures was noted to be analogous to that of a pure Au particle. A similar observation was also done by Guo et al. [149] with a 4 nm electrodeposited  $\text{Ni}(\text{OH})_2$  layer on nanoporous Au. The fabricated core-shell nanostructures were able to shield the active sites on the particle surface from  $\text{Cl}^-$  and intermediates adsorption. At the same time the formed Ni layer allowed the formation of metal-OH sites, similarly to the Au-OH sites at more negative potentials. In this way it was possible to avoid the oxidation of other interfering substances present in the electrolytic solution.

With the use of electrodeposition, Zhou et al. [150] constructed a NiPt nanosheet array on carbon paper and concluded that the Pt:Ni ratio which gave the highest anodic peak in alkaline solution was 1:160. For higher amounts of Pt a decrease in current was observed, likely because

the benefits in terms of improved electrical conductivity did not counterbalance the substitution of NiO(OH) centers with the less active PtOH.

Other Ni-based bimetallic nanoparticles for glucose sensing include Ag-Ni [151] for which the Ag:Ni ratio giving the strongest activity was observed to be 1:4.

In the future, Ni-noble metal systems might play a larger role in the field of continuous non enzymatic glucose monitoring devices. However most of the literature still performs the amperometric calibration in highly alkaline conditions, which is far from those of clinical applications requiring continuous glucose monitoring [105]. Therefore, a calibration in phosphate buffer solution at neutral pH should be the end-goal.

Table 4 summarizes the sensing characteristics of enzyme-free glucose sensors using bimetallic nickel-based nanomaterials.

## 7. Nickel MOF

*Metal organic frameworks* (MOFs), have emerged as a new class of materials that combine unique properties such as microporosity, high apparent surface areas, and exceptional thermal and chemical stability [152]. For all these reasons MOFs are highly attractive as potential materials for the development of sensors. However, their low electrical conductivity and instability in the aqueous media has limited their applications for electrochemical sensing [153,154]. However, enthralling opportunities are provided by the relatively novel field of conductive MOFs, which are characterized by highly conjugated and delocalized  $\pi$ -bond in the ligand. Such a structure facilitates electron transport and greatly enhances its electrical conductivity with high sensing capability [155].

In a recent work, Zeraati and colleagues synthesized a Ni-MOF with an ultrasonic assisted reverse micelle synthetic route, with a sensitivity of  $2859.95 \mu\text{A mM}^{-1} \text{cm}^{-2}$  and a LOD of  $0.76 \mu\text{M}$  [156]. Using a facile one pot solution process Xiao et al. [157] demonstrated that the Ni-MOF nanobelt morphology is favorable to glucose oxidation, in particular due to its reduced thickness which maximizes the surface area.

An interesting avenue, proposed by Wang et al. [158], consists in the combination of a hierarchical flower-like Ni-MOF with single walled carbon nanotubes (SWCNT) used to enhance the electrical conductivity. The authors noted that the addition of the SWCNT not only led to an increase in faradaic current density but also led to a decrease in the peak-to-peak distance for the Ni(II)/Ni(III) couple suggesting an improvement also in the electrochemical reversibility. Analogously, Zhang et al. [159] achieved an extremely high sensitivity of  $13850 \mu\text{A mM}^{-1} \text{cm}^{-2}$  by combining a Ni-MOF with carbon nanotubes. An even greater sensitivity of  $21744 \mu\text{A mM}^{-1} \text{cm}^{-2}$  was reported by Qiao et al. [160] for a Ni-MOF synthesized via solvothermal methods on carbon cloth.

With an exciting approach, Xue et al. [161] fabricated a 2D Ni@Cu-MOF by simple room temperature stirring. After performing electrochemical impedance spectroscopy analysis, the researchers concluded that the addition of Ni to the Cu-MOF caused an overall decrease in electrical resistivity. The as obtained sensor showed a sensitivity of  $1703 \mu\text{A mM}^{-1} \text{cm}^{-2}$  and a LOD of  $1.67 \mu\text{M}$  in 0.1 M NaOH. In an comparable study, Kim et al. [162] developed a Ni@Cu MOF through a two-step hydrothermal method.

Bimetallic MOF based on Co have also been synthesized with different morphologies and supports [163,164], due to the notable performance afforded by the synergistic interactions between the two metals.

As an example, in the solution proposed by Xu et al. [165], a nanorod-like bimetallic Ni/Co MOF was grown on a carbon cloth support. The sensor boasted a high sensitivity of  $3250 \mu\text{A mM}^{-1} \text{cm}^{-2}$  and a low LOD of  $0.1 \mu\text{M}$ . The authors attributed the notable performance to the Ni/Co synergy and to the high surface area of the open framework structure. Cao and colleagues [166] investigated the effect of the

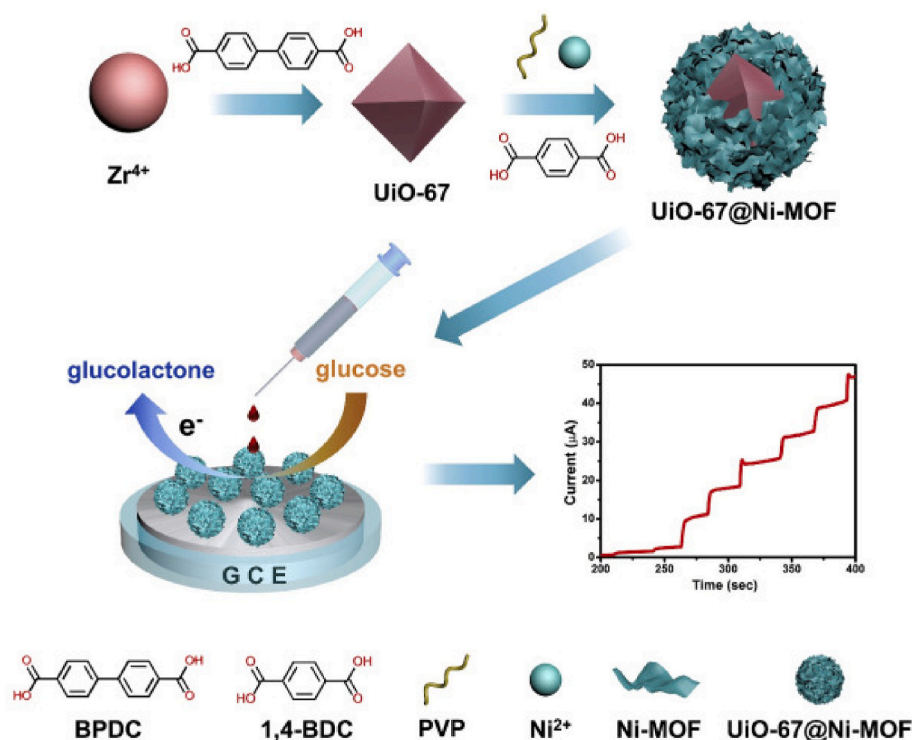


**Fig. 11.** Schematic illustration of the synthesis of core-shell UiO-67@Ni-MOF composites by internal extended growth under polyvinylpyrrolidone regulation and non-enzymatic sensing of glucose by UiO-67@Ni-MOF-modified electrode. Reproduced from Ref. [167] with permission from Elsevier.

**Table 5**

Comparison table for nickel MOF-based electrochemical non-enzymatic glucose sensors.

Electrode	Solution	Linear range ( $\mu M$ )	LOD ( $\mu M$ )	Sensitivity ( $\mu A\text{ mM}^{-1}\text{ cm}^{-2}$ )	Ref.
Ni-MOF	0.1 M NaOH	1–1600	0.76	2860	[156]
Ni-MOF	0.1 M NaOH	1–500	0.66	21744	[160]
Ni-MOF/GCE	0.1 M NaOH	25–3150	0.6	402	[168]
Ni-MOF/CNT	0.1 M NaOH	20–4400	4.6	–	[158]
Ni@Cu-MOF	0.1 M NaOH	5–2500	1.67	1703	[161]
Ni@Cu-MOF	0.1 M NaOH	0–5000	0.4	496	[162]
Ni@Cu-MOF	0.1 M NaOH	20–4930	15	1832	[169]
Ni@Co-MOF	0.1 M NaOH	0.3–2312	0.1	3250	[165]
Ni@Co-MOF	0.1 M KOH	1–3800	0.3	2800	[163]
Ag/Ni-MOF	0.1 M NaOH	5–500	5	160	[166]
Ni-MOF/CNT	0.2 M NaOH	1–1600	0.82	13850	[159]
Ni-MOF NB	0.1 M NaOH	1–500	0.25	1542	[157]
Ni-MOF@UiO67	0.1 M NaOH	5–3900	0.98	–	[167]

integration of Ag nanoparticles in a matrix of Ni-MOF nanosheets. Compared to other systems in the literature, their sensor displayed a lower sensitivity ( $160\ \mu A\text{ mM}^{-1}\text{ cm}^{-2}$ ).

A fascinating proposal by Lu et al. [167] consists in the use of core-shell MOF@MOF by internal extended growth of a shell of Ni-MOF on a core UiO-67. A schematic of the novel synthetic process is presented in Fig. 11. The researchers compared the electrochemical response of the composite with that of Ni-MOF and noted a decrease in the peak-to-peak distance and an increase in the glucose oxidation peak. This was attributed to the excellent electrical conductivity of UiO-67, which in turn improved the electron transfer rate constant.

Table 5 provides a summary of the sensing performance of nickel MOF-based sensors.

## 8. Conclusions

Ni-based materials are attracting the attention of the scientific community for their outstanding performance towards glucose electro-oxidation. Ni selenides, sulfides and nitrates are only recently being

studied and have already shown promising results due to their strong redox capabilities and good electrical conductivity. The combination with a conductive carbonaceous matrix to form composite electrodes is a common solution to achieve a stronger electrocatalytic response due to an improved charge transfer constant. As a general rule, the highest sensitivity values for electrodes based on Ni-based compounds are obtained when the catalyst is grown directly on a Ni foam, instead of being drop cast and/or fixed on the surface with a binder.

A promising avenue is the use of bimetallic nanosystems where Ni is a component (e.g., Cu/Ni, Co/Ni, Ag/Ni, Au/Ni and Pt/Ni) due to their superior activity, biocompatibility and fouling/poisoning resistance.

Conductive MOF with Ni centers results in strong current responses thanks to their open pore structure combined with the oxidative power of Ni(III). The integration of Ni-MOF with nano-carbon based materials significantly improves the electrical conductivity and the combination with Cu and Co engenders synergistic interactions.

## Declaration of competing interest

The authors declare that they have no known competing financial interests or personal relationships that could have appeared to influence the work reported in this paper.

## Data availability

No data was used for the research described in the article.

## References

- [1] D.J. Magliano, et al., Trends in incidence of total or type 2 diabetes: systematic review, *BMJ* 366 (Sep. 2019), 15003, <https://doi.org/10.1136/bmj.15003>.
- [2] Review of glucose Oxidases and glucose dehydrogenases: a Bird's eye view of glucose sensing enzymes - Stefano Ferri, Katsuhiko Kojima, Koji Sode (2011) accessed 07. 05, 2022, <https://journals.sagepub.com/doi/10.1177/193229681100500507>.
- [3] S.K. Vashist, D. Zheng, K. Al-Rubeaan, J.H.T. Luong, F.-S. Sheu, Technology behind commercial devices for blood glucose monitoring in diabetes management: a review, *Anal. Chim. Acta* 703 (2) (Oct. 2011) 124–136, <https://doi.org/10.1016/j.aca.2011.07.024>.
- [4] H. Teymourian, A. Barfidokht, J. Wang, Electrochemical glucose sensors in diabetes management: an updated review (2010–2020), *Chem. Soc. Rev.* 49 (21) (2020) 7671–7709, <https://doi.org/10.1039/d0cs00304b>.
- [5] D.-W. Hwang, S. Lee, M. Seo, T.D. Chung, Recent advances in electrochemical non-enzymatic glucose sensors - a review, *Anal. Chim. Acta* 1033 (Nov. 2018) 1–34, <https://doi.org/10.1016/j.aca.2018.05.051>.
- [6] H. Lee, Y.J. Hong, S. Baik, T. Hyeon, D.-H. Kim, Enzyme-based glucose sensor: from invasive to Wearable device, *Adv. Healthc. Mater.* 7 (8) (2018), 1701150, <https://doi.org/10.1002/adhm.201701150>.
- [7] K. Tian, M. Prestgard, A. Tiwari, A review of recent advances in nonenzymatic glucose sensors, *Mater. Sci. Eng. C* 41 (Aug. 2014) 100–118, <https://doi.org/10.1016/j.msec.2014.04.013>.
- [8] H. Zhu, L. Li, W. Zhou, Z. Shao, X. Chen, Advances in non-enzymatic glucose sensors based on metal oxides, *J. Mater. Chem. B* 4 (46) (2016) 7333–7349, <https://doi.org/10.1039/C6TB02037B>.
- [9] E. Sehit, Z. Altintas, Significance of nanomaterials in electrochemical glucose sensors: an updated review (2016–2020), *Biosens. Bioelectron.* 159 (Jul. 2020), 112165, <https://doi.org/10.1016/j.bios.2020.112165>.
- [10] C. He, M. Asif, Q. Liu, F. Xiao, H. Liu, and B. Y. Xia, "Noble metal construction for electrochemical nonenzymatic glucose detection," *Adv. Mater. Technol.*, vol. n/a, no. n/a, p. 2200272, doi: 10.1002/admt.202200272.
- [11] D. Pletcher, Electrocatalysis: present and future, *J. Appl. Electrochem.* 14 (4) (1984) 403–415, <https://doi.org/10.1007/bf00610805>.
- [12] L.D. Burke, Premonolayer oxidation and its role in electrocatalysis, *Electrochim. Acta* 39 (11–12) (1994) 1841–1848, [https://doi.org/10.1016/0013-4686\(94\)85173-5](https://doi.org/10.1016/0013-4686(94)85173-5).
- [13] K.E. Toghill, R.G. Compton, Electrochemical non-enzymatic glucose sensors: a perspective and an evaluation, *Int. J. Electrochem. Sci.* 5 (9) (2010) 1246–1301.
- [14] S. Park, H. Boo, T.D. Chung, Electrochemical non-enzymatic glucose sensors, *Anal. Chim. Acta* 556 (1) (Jan. 2006) 46–57, <https://doi.org/10.1016/j.aca.2005.05.080>.
- [15] S. Geiger, S. Cherevko, K.J.J. Mayrhofer, Dissolution of platinum in presence of chloride traces, *Electrochim. Acta* 179 (2015) 24–31, <https://doi.org/10.1016/j.electacta.2015.03.059>.
- [16] M. Pasta, F.L. Mantia, Y. Cui, Mechanism of glucose electrochemical oxidation on gold surface, *Electrochim. Acta* 55 (20) (2010) 5561–5568, <https://doi.org/10.1016/j.electacta.2010.04.069>.
- [17] H. Alqaralleh, A. Canepa, The role of precious metals in portfolio diversification during the Covid19 pandemic: a wavelet-based quantile approach, *Resour. Policy* 75 (Mar. 2022), 102532, <https://doi.org/10.1016/j.resourpol.2021.102532>.
- [18] Z. Cui, H. Yin, Q. Nie, D. Qin, W. Wu, X. He, Hierarchical flower-like NiO hollow microspheres for non-enzymatic glucose sensors, *J. Electroanal. Chem.* 757 (Nov. 2015) 51–57, <https://doi.org/10.1016/j.jelechem.2015.09.011>.
- [19] A. Ashok, A. Kumar, F. Tarlochan, Highly efficient nonenzymatic glucose sensors based on CuO nanoparticles, *Appl. Surf. Sci.* 481 (Jul. 2019) 712–722, <https://doi.org/10.1016/j.apsusc.2019.03.157>.
- [20] H. Xu, et al., Electrochemical non-enzymatic glucose sensor based on hierarchical 3D Co3O4/Ni heterostructure electrode for pushing sensitivity boundary to a new limit, *Sensor. Actuator. B Chem.* 267 (Aug. 2018) 93–103, <https://doi.org/10.1016/j.snb.2018.04.023>.
- [21] Y.J. Yang, J. Zi, W. Li, Enzyme-free sensing of hydrogen peroxide and glucose at a CuS nanoflowers modified glassy carbon electrode, *Electrochim. Acta* 115 (Jan. 2014) 126–130, <https://doi.org/10.1016/j.electacta.2013.10.168>.
- [22] Y. Li, Q. Xiao, S. Huang, Highly active nickel-doped FeS2 nanoparticles trigger non-enzymatic glucose detection, *Mater. Chem. Phys.* 193 (Jun. 2017) 311–315, <https://doi.org/10.1016/j.materchemphys.2017.02.051>.
- [23] R. Singh, M.M. Ayyub, Atomic layer deposition of crystalline  $\beta$ -NiS for superior sensing in thin-film non-enzymatic electrochemical glucose sensors, *ACS Appl. Electron. Mater.* 3 (4) (Apr. 2021) 1912–1919, <https://doi.org/10.1021/acsaem.1c00145>.
- [24] Y. Li, et al., Co-MOF nanosheet array: a high-performance electrochemical sensor for non-enzymatic glucose detection, *Sensor. Actuator. B Chem.* 278 (2019) 126–132, <https://doi.org/10.1016/j.snb.2018.09.076>.
- [25] X. Zhang, et al., Ultrasensitive binder-free glucose sensors based on the pyrolysis of in situ grown Cu MOF, *Sensor. Actuator. B Chem.* 254 (Jan. 2018) 272–281, <https://doi.org/10.1016/j.snb.2017.07.024>.
- [26] Y. Qiao, et al., A comparative study of electrocatalytic oxidation of glucose on conductive Ni-MOF nanosheet arrays with different ligands, *New J. Chem.* 44 (41) (2020) 17849–17853, <https://doi.org/10.1039/D0NJ04150E>.
- [27] Z. Zhu, L. Garcia-Gancedo, A.J. Flewitt, H. Xie, F. Moussy, W.I. Milne, A critical review of glucose biosensors based on carbon nanomaterials: carbon nanotubes and graphene, *Sensors* 12 (5) (May 2012) 5996–6022, <https://doi.org/10.3390/s120505996>.
- [28] P. Kannan, G. Maduraiveeran, Bimetallic nanomaterials-based electrochemical biosensor platforms for clinical applications, *Micromachines* 13 (1) (Jan. 2022), <https://doi.org/10.3390/mi13010076>. Art. no. 1.
- [29] H.L. Chia, C.C. Mayorga-Martinez, M. Pumera, Doping and decorating 2D materials for biosensing: benefits and drawbacks, *Adv. Funct. Mater.* 31 (46) (2021), 2102555, <https://doi.org/10.1002/adfm.202102555>.
- [30] S.N.A. Mohd Yazid, I. Md Isa, S. Abu Bakar, N. Hashim, S. Ab Ghani, A review of glucose biosensors based on graphene/metal oxide nanomaterials, *Anal. Lett.* 47 (11) (Jul. 2014) 1821–1834, <https://doi.org/10.1080/00032719.2014.888731>.
- [31] P. Luo, F. Zhang, R.P. Baldwin, Comparison of metallic electrodes for constant-potential amperometric detection of carbohydrates, amino acids and related compounds in flow systems, *Anal. Chim. Acta* 244 (1991) 169–178, [https://doi.org/10.1016/s0003-2670\(00\)82494-0](https://doi.org/10.1016/s0003-2670(00)82494-0).
- [32] M. Fleischmann, K. Korinek, D. Pletcher, The oxidation of organic compounds at a nickel anode in alkaline solution, *J. Electroanal. Chem. Interfacial Electrochem.* 31 (1) (Jun. 1971) 39–49, [https://doi.org/10.1016/S0022-0728\(71\)80040-2](https://doi.org/10.1016/S0022-0728(71)80040-2).
- [33] S.M. El-Refaei, M.M. Saleh, M.I. Awad, Tolerance of glucose electrocatalytic oxidation on NiOx/MnOx/GC electrode to poisoning by halides, *J. Solid State Electrochem.* 18 (1) (2014) 5–12, <https://doi.org/10.1007/s10008-013-2205-1>.
- [34] Nickel: A review of its sources and environmental toxicology," *Pol. J. Environ. Stud.*, vol. 15, no. 3, pp. 375–382.
- [35] S.Z. Tasker, E.A. Standley, T.F. Jamison, Recent advances in homogeneous nickel catalysis, *Nature* 509 (May 2014) 7500, <https://doi.org/10.1038/nature13274>. Art. no. 7500.
- [36] S. De, J. Zhang, R. Luque, N. Yan, Ni-based bimetallic heterogeneous catalysts for energy and environmental applications, *Energy Environ. Sci.* 9 (11) (Nov. 2016) 3314–3347, <https://doi.org/10.1039/C6EE02002J>.
- [37] R.E. Reim, R.M. Van Effen, Determination of carbohydrates by liquid chromatography with oxidation at a nickel(III) oxide electrode, *Anal. Chem.* 58 (14) (Dec. 1986) 3203–3207, <https://doi.org/10.1021/ac00127a062>.
- [38] C.-Y. Ko, J.-H. Huang, S. Raina, W.P. Kang, A high performance non-enzymatic glucose sensor based on nickel hydroxide modified nitrogen-incorporated nanodiamonds, *Analyst* 138 (11) (May 2013) 3201–3208, <https://doi.org/10.1039/C3AN36679K>.
- [39] N. Singer, R.G. Pillai, A.I.D. Johnson, K.D. Harris, A.B. Jemere, Nanostructured nickel oxide electrodes for non-enzymatic electrochemical glucose sensing, *Microchim. Acta* 187 (4) (Mar. 2020) 196, <https://doi.org/10.1007/s00604-020-4171-5>.
- [40] S. Berchmans, H. Gomathi, G.P. Rao, Electrooxidation of alcohols and sugars catalysed on a nickel oxide modified glassy carbon electrode, *J. Electroanal. Chem.* 394 (1) (Sep. 1995) 267–270, [https://doi.org/10.1016/0022-0728\(95\)04099-A](https://doi.org/10.1016/0022-0728(95)04099-A).
- [41] W. Visscher, E. Barendrecht, Investigation of thin-film  $\alpha$ - and  $\beta$ -Ni(OH)2 electrodes in alkaline solutions, *J. Electroanal. Chem. Interfacial Electrochem.* 154 (1) (Sep. 1983) 69–80, [https://doi.org/10.1016/S0022-0728\(83\)80532-4](https://doi.org/10.1016/S0022-0728(83)80532-4).
- [42] F. Hahn, B. Beden, M.J. Croissant, C. Lamy, In situ visible reflectance spectroscopic investigation of the nickel electrode-alkaline solution interface, *Electrochim. Acta* 31 (3) (Mar. 1986) 335–342, [https://doi.org/10.1016/0013-4686\(86\)80087-1](https://doi.org/10.1016/0013-4686(86)80087-1).
- [43] M. Wei, et al., Electrochemical non-enzymatic glucose sensors: recent progress and perspectives, *Chem. Commun.* 56 (93) (2020) 14553–14569, <https://doi.org/10.1039/D0CC05650B>.
- [44] E. Peltola, S. Sainio, K.B. Holt, T. Palomäki, J. Koskinen, T. Laurila, Electrochemical fouling of dopamine and recovery of carbon electrodes, *Anal. Chem.* 90 (2) (Jan. 2018) 1408–1416, <https://doi.org/10.1021/acs.analchem.7b04793>.
- [45] R.M. de Carvalho, R.S. Freire, S. Rath, L.T. Kubota, Effects of EDTA on signal stability during electrochemical detection of acetaminophen, *J. Pharm. Biomed. Anal.* 34 (5) (Mar. 2004) 871–878, <https://doi.org/10.1016/j.jpba.2003.11.005>.
- [46] X. Qi, R.F. Tester, Lactose, maltose, and sucrose in health and disease, *Mol. Nutr. Food Res.* 64 (8) (2020), 1901082, <https://doi.org/10.1002/mnfr.201901082>.
- [47] C. Patel, et al., Effect of dietary fructose on portal and systemic serum fructose levels in rats and in KHK-/- and GLUT5-/- mice, *Am. J. Physiol. Gastrointest. Liver Physiol.* 309 (9) (Nov. 2015) G779–G790, <https://doi.org/10.1152/ajpgi.00188.2015>.
- [48] L. Johnston, G. Wang, K. Hu, C. Qian, G. Liu, Advances in biosensors for continuous glucose monitoring towards Wearables, *Front. Bioeng. Biotechnol.* 9 (2021). Accessed: 09. 18, 2022. [Online]. Available: <https://www.frontiersin.org/articles/10.3389/fbioe.2021.733810>.
- [49] B.L. Hanssen, S. Siraj, D.K.Y. Wong, Recent strategies to minimise fouling in electrochemical detection systems, *Rev. Anal. Chem.* 35 (1) (2016) 1–28, <https://doi.org/10.1515/revac-2015-0008>.

- [50] A. Olejnik, K. Siuzdak, J. Karczewski, K. Grochowska, A flexible nafion coated enzyme-free glucose sensor based on Au-dimpled Ti structures, *Electroanalysis* 32 (2) (2020) 323–332, <https://doi.org/10.1002/elan.201900455>.
- [51] J.-C. Chou, et al., The flexible arrayed non-enzymatic CZO glucose sensor utilizing silver nanowires and nafion, *IEEE Trans. Instrum. Meas.* 70 (2021) 1–11, <https://doi.org/10.1109/TIM.2021.3099572>.
- [52] C.A. Pfortmueller, D. Uehlinger, S. von Haehling, J.C. Schefold, Serum chloride levels in critical illness—the hidden story, *Intensive Care Med.* 6 (Apr. 2018) 10, <https://doi.org/10.1186/s40635-018-0174-5>.
- [53] K. Berend, L.H. van Hulsteijn, R.O.B. Gans, Chloride: the queen of electrolytes? *Eur. J. Intern. Med.* 23 (3) (Apr. 2012) 203–211, <https://doi.org/10.1016/j.ejim.2011.11.013>.
- [54] M.W. Hsiao, R.R. Adzic, E.B. Yeager, The effects of adsorbed anions on the oxidation of D-glucose on gold single crystal electrodes, *Electrochim. Acta* 37 (2) (1992) 357–363, [https://doi.org/10.1016/0013-4686\(92\)85024-f](https://doi.org/10.1016/0013-4686(92)85024-f).
- [55] M.W. Hsiao, R.R. Adzic, E.B. Yeager, Electrochemical oxidation of glucose on single crystal and polycrystalline gold surfaces in phosphate buffer, *J. Electrochem. Soc.* 143 (3) (1996) 759–767, <https://doi.org/10.1149/1.1836536>, 759–767.
- [56] V.N. Kamath, H. Lal, Halide adsorption and the anodic oxidation of chemisorbed methanol on platinum, *J. Electroanal. Chem. Interfacial Electrochem.* 24 (1) (Jan. 1970) 125–135, [https://doi.org/10.1016/S0022-0728\(70\)80013-4](https://doi.org/10.1016/S0022-0728(70)80013-4).
- [57] J. Sobkowski, K. Franaszczuk, K. Dobrowolska, Effect of anions and pH on the adsorption and oxidation of methanol on a platinum electrode, *J. Electroanal. Chem.* 330 (1) (Jul. 1992) 529–540, [https://doi.org/10.1016/0022-0728\(92\)80329-3](https://doi.org/10.1016/0022-0728(92)80329-3).
- [58] E.B. Makovos, C.C. Liu, A cyclic-voltammetric study of glucose oxidation on a gold electrode, *Bioelectrochem.* 15 (2) (1986) 157–165, [https://doi.org/10.1016/0302-4598\(86\)80023-x](https://doi.org/10.1016/0302-4598(86)80023-x).
- [59] P. Marcus, *Corrosion Mechanisms in Theory and Practice*, third ed., CRC Press, 2011.
- [60] S. Luo, et al., A new method for fabricating a CuO/TiO<sub>2</sub> nanotube arrays electrode and its application as a sensitive nonenzymatic glucose sensor, *Talanta* 86 (Oct. 2011) 157–163, <https://doi.org/10.1016/j.talanta.2011.08.051>.
- [61] Y. Liu, H. Teng, H. Hou, T. You, Nonenzymatic glucose sensor based on renewable electrospun Ni nanoparticle-loaded carbon nanofiber paste electrode, *Biosens. Bioelectron.* 24 (11) (2009) 3329–3334, <https://doi.org/10.1016/j.bios.2009.04.032>.
- [62] D.M. Novak, B.E. Conway, Competitive adsorption and state of charge of halide ions in monolayer oxide film growth processes at Pt anodes, *J. Chem. Soc. Faraday Trans. 1 Phys. Chem. Condens. Phases* 77 (10) (Jan. 1981) 2341–2359, <https://doi.org/10.1039/F19817702341>.
- [63] A. Bouzoubaa, D. Costa, B. Diawara, N. Audiffren, P. Marcus, Insight of DFT and atomistic thermodynamics on the adsorption and insertion of halides onto the hydroxylated NiO(111) surface, *Corrosion Sci.* 52 (8) (2010) 2643–2652, <https://doi.org/10.1016/j.corsci.2010.04.014>.
- [64] N. Pineau, C. Minot, V. Maurice, P. Marcus, Density functional theory study of the interaction of Cl<sup>-</sup> with passivated nickel surfaces, *Electrochim. Solid State Lett.* 6 (11) (Aug. 2003) B47, <https://doi.org/10.1149/1.1612012>.
- [65] L. Pauling, *The Nature of the Chemical Bond: and the Structure of Molecules and Crystals; an Introduction to Modern Structural Chemistry*, 1940.
- [66] J. Suntivich, K.J. May, H.A. Gasteiger, J.B. Goodenough, Y. Shao-Horn, A perovskite oxide optimized for oxygen evolution catalysis from molecular Orbital principles, *Science* 334 (6061) (Dec. 2011) 1383–1385, <https://doi.org/10.1126/science.1212858>.
- [67] R.A. Hussain, I. Hussain, Fabrication and applications of nickel selenide, *J. Solid State Chem.* 277 (Sep. 2019) 316–328, <https://doi.org/10.1016/j.jssc.2019.06.015>.
- [68] T. Lu, S. Dong, C. Zhang, L. Zhang, G. Cui, Fabrication of transition metal selenides and their applications in energy storage, *Coord. Chem. Rev.* 332 (Feb. 2017) 75–99, <https://doi.org/10.1016/j.ccr.2016.11.005>.
- [69] A. Sivanantham, S. Shanmugam, Nickel selenide supported on nickel foam as an efficient and durable non-precious electrocatalyst for the alkaline water electrolysis, *Appl. Catal. B Environ.* 203 (Apr. 2017) 485–493, <https://doi.org/10.1016/j.apcatb.2016.10.050>.
- [70] H. Ren, Z.-H. Huang, Z. Yang, S. Tang, F. Kang, R. Lv, Facile synthesis of free-standing nickel chalcogenide electrodes for overall water splitting, *J. Energy Chem.* 26 (6) (Nov. 2017) 1217–1222, <https://doi.org/10.1016/j.jechem.2017.10.004>.
- [71] C. Tang, et al., In situ growth of NiSe nanowire film on nickel foam as an electrode for high-performance supercapacitors, *Chemelectrochem* 2 (12) (2015) 1903–1907, <https://doi.org/10.1002/celec.201500285>.
- [72] K. Xu, et al., Solution-liquid-solid synthesis of hexagonal nickel selenide nanowire arrays with a nonmetal catalyst, *Angew. Chem.* 128 (5) (2016) 1742–1745, <https://doi.org/10.1002/ange.201508704>.
- [73] H. Sun, et al., Fabrication of NiSe<sub>2</sub> by direct selenylation of a nickel surface, *Appl. Surf. Sci.* 428 (Jan. 2018) 623–629, <https://doi.org/10.1016/j.apsusc.2017.09.201>.
- [74] S. Mani, S. Ramaraj, S.-M. Chen, B. Dinesh, T.-W. Chen, Two-dimensional metal chalcogenides analogous NiSe<sub>2</sub> nanosheets and its efficient electrocatalytic performance towards glucose sensing, *J. Colloid Interface Sci.* 507 (Dec. 2017) 378–385, <https://doi.org/10.1016/j.jcis.2017.08.018>.
- [75] Z. Xu, Q. Wang, R. Li, H. Zhangsun, M. Dong, L. Wang, Surface selenylation engineering for construction of a hierarchical NiSe<sub>2</sub>/carbon nanorod: a high-performance nonenzymatic glucose sensor, *ACS Appl. Mater. Interfaces* 13 (19) (May 2021) 22866–22873, <https://doi.org/10.1021/acsami.1c04831>.
- [76] Design and application of foams for electrocatalysis - zhu - 2017 - ChemCatChem - Wiley online library, accessed 06. 28, 2022, <https://chemistry-europe.onlinelibrary.wiley.com/doi/10.1002/cctc.201601607>.
- [77] M. Ma, et al., Surface engineering of nickel selenide nanosheets array on nickel foam: an integrated anode for glucose sensing, *Sensor. Actuator. B Chem.* 278 (Jan. 2019) 110–116, <https://doi.org/10.1016/j.snb.2018.09.075>.
- [78] S. Kukulnuri, M. Reshma Krishnan, S. Sampath, The effect of structural dimensionality on the electrocatalytic properties of the nickel selenide phase, *Phys. Chem. Chem. Phys.* 17 (36) (2015) 23448–23459, <https://doi.org/10.1039/C5CP03900B>.
- [79] N. Vishnu, P. Sahatiya, C.Y. Kong, S. Badhulika, Large area, one step synthesis of NiSe<sub>2</sub> films on cellulose paper for glucose monitoring in bio-mimicking samples for clinical diagnostics, *Nanotechnology* 30 (35) (Jun. 2019), 355502, <https://doi.org/10.1088/1361-6528/ab2008>.
- [80] H. Sabeeh, et al., Self-supporting design of NiS/CNTs nanohybrid for advanced electrochemical energy storage applications, *J. Clust. Sci.*, Jul. (2021), <https://doi.org/10.1007/s10876-021-02138-w>.
- [81] J.-H. Wang, Z. Cheng, J.-L. Brédas, M. Liu, Electronic and vibrational properties of nickel sulfides from first principles, *J. Chem. Phys.* 127 (21) (Dec. 2007), 214705, <https://doi.org/10.1063/1.2801985>.
- [82] Y. Pan, Y. Chen, X. Li, Y. Liu, C. Liu, Nanostructured nickel sulfides: phase evolution, characterization and electrocatalytic properties for the hydrogen evolution reaction, *RSC Adv.* 5 (127) (2015) 104740–104749, <https://doi.org/10.1039/C5RA18737K>.
- [83] W. Maiaugree, A. Tangtrakarn, S. Lowpa, N. Ratchapolthavisin, V. Amornkitbamrung, Facile synthesis of bilayer carbon/Ni3S2 nanowalls for a counter electrode of dye-sensitized solar cell, *Electrochim. Acta* 174 (Aug. 2015) 955–962, <https://doi.org/10.1016/j.electacta.2015.06.051>.
- [84] M. Kumar, D.I. Jeong, N. Sarwar, D.H. Yoon, Ni3S2 Heazlewoodite, An electroactive material for supercapacitor application, *Ceram. Int.* 47 (12) (Jun. 2021) 16852–16860, <https://doi.org/10.1016/j.ceramint.2021.02.260>.
- [85] P.K. Kannan, C.S. Rout, High performance non-enzymatic glucose sensor based on one-step electrodeposited nickel sulfide, *Chem. Eur. J.* 21 (26) (2015) 9355–9359, <https://doi.org/10.1002/chem.201500851>.
- [86] B.T. Zhu, Z. Wang, S. Ding, J.S. Chen, X.W. David Lou, Hierarchical nickel sulfide hollow spheres for high performance supercapacitors, *RSC Adv.* 1 (3) (Sep. 2011) 397–400, <https://doi.org/10.1039/C1RA00240F>.
- [87] C. Wei, et al., NiS hollow spheres for high-performance supercapacitors and non-enzymatic glucose sensors, *Chem. Asian J.* 10 (3) (2015) 679–686, <https://doi.org/10.1002/asia.201403198>.
- [88] S. Kubendhiran, R. Sakthivel, S.-M. Chen, B. Mutharani, Functionalized-carbon black as a conductive matrix for nickel sulfide nanospheres and its application to non-enzymatic glucose sensor, *J. Electrochem. Soc.* 165 (3) (Feb. 2018) B96, <https://doi.org/10.1149/2.0451803jes>.
- [89] T.-W. Lin, C.-J. Liu, C.-S. Dai, Ni3S2/carbon nanotube nanocomposite as electrode material for hydrogen evolution reaction in alkaline electrolyte and enzyme-free glucose detection, *Appl. Catal. B Environ.* 154 (155) (Jul. 2014) 213–220, <https://doi.org/10.1016/j.apcatb.2014.02.017>.
- [90] A. Meng, et al., Nickel sulfide nanoworm network architecture as a binder-free high-performance non-enzymatic glucose sensor, *Microchim. Acta* 188 (2) (Jan. 2021) 34, <https://doi.org/10.1007/s00604-020-04665-1>.
- [91] H. Huo, Y. Zhao, C. Xu, 3D Ni3S2 nanosheet arrays supported on Ni foam for high-performance supercapacitor and non-enzymatic glucose detection, *J. Mater. Chem.* 2 (36) (Aug. 2014) 15111–15117, <https://doi.org/10.1039/C4TA02857K>.
- [92] S. Kim, S.H. Lee, M. Cho, Y. Lee, Solvent-assisted morphology confinement of a nickel sulfide nanostructure and its application for non-enzymatic glucose sensor, *Biosens. Bioelectron.* 85 (Nov. 2016) 587–595, <https://doi.org/10.1016/j.bios.2016.05.062>.
- [93] S. Radhakrishnan, S.J. Kim, Facile fabrication of NiS and a reduced graphene oxide hybrid film for nonenzymatic detection of glucose, *RSC Adv.* 5 (55) (May 2015) 44346–44352, <https://doi.org/10.1039/C5RA01074H>.
- [94] S.H. Gage, B.G. Trewyn, C.V. Ciobanu, S. Pylpenko, R.M. Richards, Synthetic advancements and catalytic applications of nickel nitride, *Catal. Sci. Technol.* 6 (12) (Jun. 2016) 4059–4076, <https://doi.org/10.1039/C6CY00712K>.
- [95] K. Xu, et al., Metallic nickel nitride nanosheets realizing enhanced electrochemical water oxidation, *J. Am. Chem. Soc.* 137 (12) (Apr. 2015) 4119–4125, <https://doi.org/10.1021/ja5119495>.
- [96] Z. Xing, Q. Li, D. Wang, X. Yang, X. Sun, Self-supported nickel nitride as an efficient high-performance three-dimensional cathode for the alkaline hydrogen evolution reaction, *Electrochim. Acta* 191 (Feb. 2016) 841–845, <https://doi.org/10.1016/j.electacta.2015.12.174>.
- [97] N. Pandey, M. Gupta, J. Stahn, Study of reactively sputtered nickel nitride thin films, *J. Alloys Compd.* 851 (Jan. 2021), 156299, <https://doi.org/10.1016/j.jallcom.2020.156299>.
- [98] Z. Li, R.G. Gordon, V. Pallem, H. Li, D.V. Shenai, Direct-liquid-injection chemical vapor deposition of nickel nitride films and their reduction to nickel films, *Chem. Mater.* 22 (10) (May 2010) 3060–3066, <https://doi.org/10.1021/cm903636j>.
- [99] R.S. Ningthoujam, N.S. Gajbhiye, S. Sharma, Reduction mechanism of Ni<sup>2+</sup> into Ni nanoparticles prepared from different precursors: magnetic studies, *Pramana* 72 (3) (Mar. 2009) 577–586, <https://doi.org/10.1007/s12043-009-0051-6>.
- [100] F. Kahraman, S. Karadeniz, Characterization and wear behavior of plasma nitrided nickel based dental alloy, *Plasma Chem. Plasma Process.* 31 (4) (Aug. 2011) 595–604, <https://doi.org/10.1007/s11090-011-9301-8>.

- [101] J. Choi, E.G. Gillan, Solvothermal metal azide decomposition routes to nanocrystalline metastable nickel, iron, and manganese nitrides, *Inorg. Chem.* 48 (10) (May 2009) 4470–4477, <https://doi.org/10.1021/ic900260u>.
- [102] Z. Wang, W. Yu, J. Chen, M. Zhang, W. Li, K. Tao, Facile synthesis of a metastable nanocrystalline Ni<sub>3</sub>N from nickel nanoparticle, *J. Alloys Compd.* 466 (1) (Oct. 2008) 352–355, <https://doi.org/10.1016/j.jallcom.2007.11.031>.
- [103] W. Yang, S. Rehman, X. Chu, Y. Hou, S. Gao, Transition metal (Fe, Co and Ni) carbide and nitride nanomaterials: structure, chemical synthesis and applications, *ChemNanoMat* 1 (6) (2015) 376–398, <https://doi.org/10.1002/cnma.201500073>.
- [104] F. Xie, T. Liu, L. Xie, X. Sun, Y. Luo, Metallic nickel nitride nanosheet: an efficient catalyst electrode for sensitive and selective non-enzymatic glucose sensing, *Sensor. Actuator. B Chem.* 255 (Feb. 2018) 2794–2799, <https://doi.org/10.1016/j.snb.2017.09.095>.
- [105] A.D. Association, Diagnosis and classification of diabetes Mellitus, *Diabetes Care* 28 (1) (Jan. 2005) S37–S42, <https://doi.org/10.2337/diacare.28.suppl.1.S37>.
- [106] Y. Song, D. Cho, S. Venkateswarlu, M. Yoon, Systematic study on preparation of copper nanoparticle embedded porous carbon by carbonization of metal–organic framework for enzymatic glucose sensor, *RSC Adv.* 7 (17) (2017) 10592–10600, <https://doi.org/10.1039/C7RA00115K>.
- [107] X. Zeng, Y. Zhang, X. Du, Y. Li, W. Tang, A highly sensitive glucose sensor based on a gold nanoparticles/polyaniline/multi-walled carbon nanotubes composite modified glassy carbon electrode, *New J. Chem.* 42 (14) (2018) 11944–11953, <https://doi.org/10.1039/C7NJ04327A>.
- [108] X. Lin, Y. Wang, M. Zou, T. Lan, Y. Ni, Electrochemical non-enzymatic glucose sensors based on nano-composite of Co<sub>3</sub>O<sub>4</sub> and multiwalled carbon nanotube, *Chin. Chem. Lett.* 30 (6) (Jun. 2019) 1157–1160, <https://doi.org/10.1016/j.ccl.2019.04.009>.
- [109] T. Liu, M. Li, P. Dong, Y. Zhang, M. Zhou, Designing and synthesizing various nickel nitride (Ni<sub>3</sub>N) nanosheets dispersed carbon nanomaterials with different structures and porosities as the high-efficiency non-enzymatic sensors, *Sensor. Actuator. B Chem.* 260 (May 2018) 962–975, <https://doi.org/10.1016/j.snb.2018.01.076>.
- [110] M. Chen, J. Qi, D. Guo, H. Lei, W. Zhang, R. Cao, Facile synthesis of sponge-like Ni<sub>3</sub>N/NC for electrocatalytic water oxidation, *Chem. Commun.* 53 (69) (Aug. 2017) 9566–9569, <https://doi.org/10.1039/C7CC05172G>.
- [111] J. Chen, et al., Non-enzymatic glucose sensor based on nickel nitride decorated nitrogen doped carbon spheres (Ni<sub>3</sub>N/NCS) via facile one pot nitridation process, *J. Alloys Compd.* 797 (Aug. 2019) 922–930, <https://doi.org/10.1016/j.jallcom.2019.05.234>.
- [112] X. Dai, W. Deng, C. You, Z. Shen, X. Xiong, X. Sun, A Ni<sub>3</sub>N-Co<sub>3</sub>N hybrid nanowire array electrode for high-performance nonenzymatic glucose detection, *Anal. Methods* 10 (15) (2018) 1680–1684, <https://doi.org/10.1039/C8AY00370J>.
- [113] D. Yin, X. Bo, J. Liu, L. Guo, A novel enzyme-free glucose and H<sub>2</sub>O<sub>2</sub> sensor based on 3D graphene aerogels decorated with Ni<sub>3</sub>N nanoparticles, *Anal. Chim. Acta* 1038 (Dec. 2018) 11–20, <https://doi.org/10.1016/j.aca.2018.06.086>.
- [114] T. Deepalakshmi, D.T. Tran, N.H. Kim, K.T. Chong, J.H. Lee, Nitrogen-doped graphene-encapsulated nickel cobalt nitride as a highly sensitive and selective electrode for glucose and hydrogen peroxide sensing applications, *ACS Appl. Mater. Interfaces* 10 (42) (Oct. 2018) 35847–35858, <https://doi.org/10.1021/acsmi.8b15069>.
- [115] J. Chen, et al., Hybrid Ni<sub>3</sub>N-nitrogen-doped carbon microspheres (Ni<sub>3</sub>N@C) in situ derived from Ni-MOFs as sensitive non-enzymatic glucose sensors, *Mater. Technol.* 36 (5) (Apr. 2021) 286–295, <https://doi.org/10.1080/10667857.2020.1751471>.
- [116] G. Li, et al., Bimetallic nanocrystals: structure, controllable synthesis and applications in catalysis, energy and sensing, *Nanomaterials* 11 (8) (Aug. 2021), <https://doi.org/10.3390/nano11081926>. Art. no. 8.
- [117] P. Kannan, G. Maduraiveeran, Bimetallic nanomaterials-based electrochemical biosensor platforms for clinical applications, *Micromachines* 13 (1) (Jan. 2022), <https://doi.org/10.3390/mi13010076>. Art. no. 1.
- [118] R. Stephanie, M.W. Kim, S.H. Kim, J.-K. Kim, C.Y. Park, T.J. Park, Recent advances of bimetallic nanomaterials and its nanocomposites for biosensing applications, *TrAC, Trends Anal. Chem.* 135 (Feb. 2021), 116159, <https://doi.org/10.1016/j.trac.2020.116159>.
- [119] B. Hammer, J.K. Nørskov, Theoretical surface science and catalysis—calculations and concepts, *Adv. Catal.* 45 (2000) 71–129, [https://doi.org/10.1016/s0360-0564\(02\)45013-4](https://doi.org/10.1016/s0360-0564(02)45013-4).
- [120] M. Mavrikakis, B. Hammer, J.K. Nørskov, Effect of strain on the reactivity of metal surfaces, *Phys. Rev. Lett.* 81 (13) (Sep. 1998) 2819–2822, <https://doi.org/10.1103/PhysRevLett.81.2819>.
- [121] J.R. Kitchin, J.K. Nørskov, M.A. Barteau, J.G. Chen, Role of strain and ligand effects in the modification of the electronic and chemical properties of bimetallic surfaces, *Phys. Rev. Lett.* 93 (15) (Oct. 2004), 156801, <https://doi.org/10.1103/PhysRevLett.93.156801>.
- [122] J.R. Kitchin, J.K. Nørskov, M.A. Barteau, J.G. Chen, Modification of the surface electronic and chemical properties of Pt(111) by subsurface 3d transition metals, *J. Chem. Phys.* 120 (21) (2004) 10240–10246, <https://doi.org/10.1063/1.1737365>.
- [123] H. Xin, S. Linic, Communications: exceptions to the d-band model of chemisorption on metal surfaces: the dominant role of repulsion between adsorbate states and metal d-states, *J. Chem. Phys.* 132 (22) (Jun. 2010), 221101, <https://doi.org/10.1063/1.3437609>.
- [124] H. Xin, A. Vojvodic, J. Voss, J.K. Nørskov, F. Abild-Pedersen, Effects of d-band shape on the surface reactivity of transition-metal alloys, *Phys. Rev. B* 89 (11) (Mar. 2014), 115114, <https://doi.org/10.1103/PhysRevB.89.115114>.
- [125] Y. Wu, S. Cai, D. Wang, W. He, Y. Li, Syntheses of water-soluble octahedral, truncated octahedral, and cubic Pt–Ni nanocrystals and their structure–activity study in model hydrogenation reactions, *J. Am. Chem. Soc.* 134 (21) (May 2012) 8975–8981, <https://doi.org/10.1021/ja302606d>.
- [126] Y. Zhang, et al., Integrated Pt<sub>2</sub>Ni alloy@Pt core–shell nanoarchitectures with high electrocatalytic activity for oxygen reduction reaction, *J. Mater. Chem.* 2 (29) (Jul. 2014) 11400–11407, <https://doi.org/10.1039/C4TA00731J>.
- [127] T.O. Ely, et al., Synthesis of nickel nanoparticles. Influence of aggregation induced by modification of poly(vinylpyrrolidone) chain length on their magnetic properties, *Chem. Mater.* 11 (3) (Mar. 1999) 526–529, <https://doi.org/10.1021/cm980675p>.
- [128] G.-H. Han, et al., Facile direct seed-mediated growth of AuPt bimetallic shell on the surface of Pd nanocubes and application for direct H<sub>2</sub>O<sub>2</sub> synthesis, *Catalysts* 10 (6) (Jun. 2020), <https://doi.org/10.3390/catal10060650>. Art. no. 6.
- [129] K.D. Gilroy, P. Farzinpour, A. Sundar, R.A. Hughes, S. Neretina, Sacrificial templates for galvanic replacement reactions: design criteria for the synthesis of pure Pt nanoshells with a smooth surface morphology, *Chem. Mater.* 26 (10) (May 2014) 3340–3347, <https://doi.org/10.1021/cm501418d>.
- [130] G.-P. Jin, Y.-F. Ding, P.-P. Zheng, Electrodeposition of nickel nanoparticles on functional MWCNT surfaces for ethanol oxidation, *J. Power Sources* 166 (1) (Mar. 2007) 80–86, <https://doi.org/10.1016/j.jpowsour.2006.12.087>.
- [131] Y. Zhang, Y. Yang, P. Xiao, X. Zhang, L. Lu, L. Li, Preparation of Ni nanoparticle–TiO<sub>2</sub> nanotube composite by pulse electrodeposition, *Mater. Lett.* 63 (28) (Nov. 2009) 2429–2431, <https://doi.org/10.1016/j.matlet.2009.08.019>.
- [132] Y. Zhao, Y. E, L. Fan, Y. Qiu, S. Yang, A new route for the electrodeposition of platinum–nickel alloy nanoparticles on multi-walled carbon nanotubes, *Electrochim. Acta* 52 (19) (May 2007) 5873–5878, <https://doi.org/10.1016/j.electacta.2007.03.020>.
- [133] D.-H. Chen, S.-H. Wu, Synthesis of nickel nanoparticles in water-in-Oil microemulsions, *Chem. Mater.* 12 (5) (May 2000) 1354–1360, <https://doi.org/10.1021/cm991167y>.
- [134] Y. Hou, H. Kondoh, T. Ohta, S. Gao, Size-controlled synthesis of nickel nanoparticles, *Appl. Surf. Sci.* 241 (1) (Feb. 2005) 218–222, <https://doi.org/10.1016/j.apsusc.2004.09.045>.
- [135] L. Karam, J. Reboul, N. El Hassan, J. Nelayah, P. Massiani, Nanostructured nickel aluminate as a key intermediate for the production of highly dispersed and stable nickel nanoparticles supported within mesoporous alumina for dry reforming of methane, *Molecules* 24 (22) (Jan. 2019), <https://doi.org/10.3390/molecules24224107>. Art. no. 22.
- [136] I.-H. Yeo, D.C. Johnson, Anodic response of glucose at copper-based alloy electrodes, *J. Electroanal. Chem.* 484 (2) (Apr. 2000) 157–163, [https://doi.org/10.1016/S0022-0728\(00\)00072-3](https://doi.org/10.1016/S0022-0728(00)00072-3).
- [137] X. Gao, et al., Rapid fabrication of superhydrophilic micro/nanostructured nickel foam toward high-performance glucose sensor, *Adv. Mater. Interfac.* 8 (7) (2021), 2002133, <https://doi.org/10.1002/admi.202002133>.
- [138] H. Wei, et al., Dendritic core-shell copper-nickel alloy@metal oxide for efficient non-enzymatic glucose detection, *Sensor. Actuator. B Chem.* 337 (Jun. 2021), 129687, <https://doi.org/10.1016/j.snb.2021.129687>.
- [139] S. Bilal, W. Ullah, A.-H. Ali Shah, Polyaniline@CuNi nanocomposite: a highly selective, stable and efficient electrode material for binder free non-enzymatic glucose sensor, *Electrochim. Acta* 284 (Sep. 2018) 382–391, <https://doi.org/10.1016/j.electacta.2018.07.165>.
- [140] K.-C. Lin, Y.-C. Lin, S.-M. Chen, A highly sensitive nonenzymatic glucose sensor based on multi-walled carbon nanotubes decorated with nickel and copper nanoparticles, *Electrochim. Acta* 96 (Apr. 2013) 164–172, <https://doi.org/10.1016/j.electacta.2013.02.098>.
- [141] S. Ammara, S. Shamaila, N. zafari, A. Bokhari, A. Sabah, Nonenzymatic glucose sensor with high performance electrodeposited nickel/copper/carbon nanotubes nanocomposite electrode, *J. Phys. Chem. Solid.* 120 (Sep. 2018) 12–19, <https://doi.org/10.1016/j.jpjcs.2018.04.015>.
- [142] X. Xu, et al., Non-enzymatic electrochemical detection of glucose using Ni–Cu bimetallic alloy nanoparticles loaded on reduced graphene oxide through a one-step synthesis strategy, *Anal. Methods* 13 (46) (Dec. 2021) 5628–5637, <https://doi.org/10.1039/D1AY01357B>.
- [143] G.A. Naikoo, et al., Recent advances in non-enzymatic glucose sensors based on metal and metal oxide nanostructures for diabetes management- A review, *Front. Chem.* 9 (2021). Accessed: 06. 30, 2022. [Online]. Available: <https://www.frontiersin.org/article/10.3389/fchem.2021.748957>.
- [144] M. Pak, A. Moshaii, M. Nikkhah, S. Abbasian, H. Siampour, Nickel-gold bimetallic nanostructures with the improved electrochemical performance for non-enzymatic glucose determination, *J. Electroanal. Chem.* 900 (Nov. 2021), 115729, <https://doi.org/10.1016/j.jelechem.2021.115729>.
- [145] J. Zhou, et al., Electrodeposition of bimetallic NiAu alloy dendrites on carbon papers as highly sensitive disposable non-enzymatic glucose sensors, *Mater. Lett.* 273 (Aug. 2020), 127912, <https://doi.org/10.1016/j.matlet.2020.127912>.
- [146] L. Qin, L. He, J. Zhao, B. Zhao, Y. Yin, Y. Yang, Synthesis of Ni/Au multilayer nanowire arrays for ultrasensitive non-enzymatic sensing of glucose, *Sensor. Actuator. B Chem.* 240 (Mar. 2017) 779–784, <https://doi.org/10.1016/j.snb.2016.09.041>.
- [147] K. Yao, et al., Fabrication of Au/Ni/boron-doped diamond electrodes via hydrogen plasma etching graphite and amorphous boron for efficient non-enzymatic sensing of glucose, *J. Electroanal. Chem.* 871 (Aug. 2020), 114264, <https://doi.org/10.1016/j.jelechem.2020.114264>.

- [148] X. Gao, X. Du, D. Liu, H. Gao, P. Wang, J. Yang, Core-shell gold-nickel nanostructures as highly selective and stable nonenzymatic glucose sensor for fermentation process, *Sci. Rep.* 10 (1) (2020) 1365, <https://doi.org/10.1038/s41598-020-58403-x>.
- [149] M. Guo, X. Yin, C. Zhou, Y. Xia, W. Huang, Z. Li, Ultrasensitive nonenzymatic sensing of glucose on Ni(OH)<sub>2</sub>-coated nanoporous gold film with two pairs of electron mediators, *Electrochim. Acta* 142 (Oct. 2014) 351–358, <https://doi.org/10.1016/j.electacta.2014.07.135>.
- [150] J. Zhou, et al., Electrodeposition of bimetallic NiPt nanosheet arrays on carbon papers for high performance nonenzymatic disposable glucose sensors, *J. Mater. Sci. Mater. Electron.* 32 (17) (Sep. 2021) 22493–22505, <https://doi.org/10.1007/s10854-021-06735-3>.
- [151] Y. Miao, J. Wu, S. Zhou, Z. Yang, R. Ouyang, Synergistic effect of bimetallic Ag and Ni alloys on each Other's electrocatalysis to glucose oxidation, *J. Electrochem. Soc.* 160 (4) (Feb. 2013) B47, <https://doi.org/10.1149/2.059304jes>.
- [152] J.L.C. Rowsell, O.M. Yaghi, Metal-organic frameworks: a new class of porous materials, *Microporous Mesoporous Mater.* 73 (1) (Aug. 2004) 3–14, <https://doi.org/10.1016/j.micromeso.2004.03.034>.
- [153] W.-H. Li, et al., Conductive metal-organic framework nanowire arrays for electrocatalytic oxygen evolution, *J. Mater. Chem.* 7 (17) (Apr. 2019) 10431–10438, <https://doi.org/10.1039/C9TA02169H>.
- [154] Z. Liang, R. Zhao, T. Qiu, R. Zou, Q. Xu, Metal-organic framework-derived materials for electrochemical energy applications, *EnergyChem* 1 (1) (Jul. 2019), 100001, <https://doi.org/10.1016/j.enchem.2019.100001>.
- [155] L.S. Xie, G. Skorupskii, M. Dincă, Electrically conductive metal-organic frameworks, *Chem. Rev.* 120 (16) (2020) 8536–8580, <https://doi.org/10.1021/acs.chemrev.9b00766>.
- [156] M. Zeraati, V. Alizadeh, P. Kazemzadeh, M. Safinejad, H. Kazemian, G. Sargazi, A new nickel metal organic framework (Ni-MOF) porous nanostructure as a potential novel electrochemical sensor for detecting glucose, *J. Porous Mater.* 29 (1) (Feb. 2022) 257–267, <https://doi.org/10.1007/s10934-021-01164-3>.
- [157] X. Xiao, et al., Facile synthesis of ultrathin Ni-MOF nanobelts for high-efficiency determination of glucose in human serum, *J. Mater. Chem. B* 5 (26) (2017) 5234–5239, <https://doi.org/10.1039/C7TB00180K>.
- [158] F. Wang, X. Chen, L. Chen, J. Yang, Q. Wang, High-performance non-enzymatic glucose sensor by hierarchical flower-like nickel(II)-based MOF/carbon nanotubes composite, *Mater. Sci. Eng. C* 96 (Mar. 2019) 41–50, <https://doi.org/10.1016/j.msec.2018.11.004>.
- [159] X. Zhang, Y. Xu, B. Ye, An efficient electrochemical glucose sensor based on porous nickel-based metal organic framework/carbon nanotubes composite (Ni-MOF/CNTs), *J. Alloys Compd.* 767 (Oct. 2018) 651–656, <https://doi.org/10.1016/j.jallcom.2018.07.175>.
- [160] Y. Qiao, et al., High-performance non-enzymatic glucose detection: using a conductive Ni-MOF as an electrocatalyst, *J. Mater. Chem. B* 8 (25) (Jul. 2020) 5411–5415, <https://doi.org/10.1039/D0TB00131G>.
- [161] Z. Xue, L. Jia, R.-R. Zhu, L. Du, Q.-H. Zhao, High-performance non-enzymatic glucose electrochemical sensor constructed by transition nickel modified Ni@Cu-MOF, *J. Electroanal. Chem.* 858 (Feb. 2020), 113783, <https://doi.org/10.1016/j.jelechem.2019.113783>.
- [162] S. eun Kim, A. Muthurasu, Metal-organic framework-assisted bimetallic Ni@Cu microsphere for enzyme-free electrochemical sensing of glucose, *J. Electroanal. Chem.* 873 (Sep. 2020), 114356, <https://doi.org/10.1016/j.jelechem.2020.114356>.
- [163] S. Li, X. Zhan, W. Bai, J. Zheng, Controllable synthesis of Ni/Co-TCPP MOFs with different morphologies and their application in electrochemical detection of glucose, *J. Electrochem. Soc.* 167 (12) (Aug. 2020), 127506, <https://doi.org/10.1149/1945-7111/abac2a>.
- [164] W. Li, S. Lv, Y. Wang, L. Zhang, X. Cui, Nanoporous gold induced vertically standing 2D NiCo bimetal-organic framework nanosheets for non-enzymatic glucose biosensing, *Sensor. Actuator. B Chem.* 281 (Feb. 2019) 652–658, <https://doi.org/10.1016/j.snb.2018.10.150>.
- [165] Z. Xu, Q. Wang, H. Zhangsun, S. Zhao, Y. Zhao, L. Wang, Carbon cloth-supported nanorod-like conductive Ni/Co bimetal MOF: a stable and high-performance enzyme-free electrochemical sensor for determination of glucose in serum and beverage, *Food Chem.* 349 (Jul. 2021), 129202, <https://doi.org/10.1016/j.foodchem.2021.129202>.
- [166] J. Cao, J. Yun, N. Zhang, Y. Wei, H. Yang, Z. Xu, Bifunctional Ag@Ni-MOF for high performance supercapacitor and glucose sensor, *Synth. Met.* 282 (Dec. 2021), 116931, <https://doi.org/10.1016/j.synthmet.2021.116931>.
- [167] M. Lu, et al., Core-shell MOF@MOF composites for sensitive nonenzymatic glucose sensing in human serum, *Anal. Chim. Acta* 1110 (May 2020) 35–43, <https://doi.org/10.1016/j.aca.2020.02.023>.
- [168] A. Koyappayil, S. Yeon, S.G. Chavan, L. Jin, A. Go, M.-H. Lee, Efficient and rapid synthesis of ultrathin nickel-metal organic framework nanosheets for the sensitive determination of glucose, *Microchem. J.* 179 (Aug. 2022), 107462, <https://doi.org/10.1016/j.microc.2022.107462>.
- [169] W. Pan, et al., Facile synthesis of 2D/3D hierarchical NiCu bimetallic MOF for non-enzymatic glucose sensor, *Microchem. J.* 170 (Nov. 2021), 106652, <https://doi.org/10.1016/j.microc.2021.106652>.